Modern Methods in Heterogeneous Catalysis Research

Solid State Aspects in Oxidation Catalysis

20th January 2012

Maik Eichelbaum / FHI

How chemists like to see the world:
Everything is molecular

Top Catal (2008) 50:98–105

How Far is the Concept of Isolated Active Sites Valid in Solid Catalysts?

John Meurig Thomas

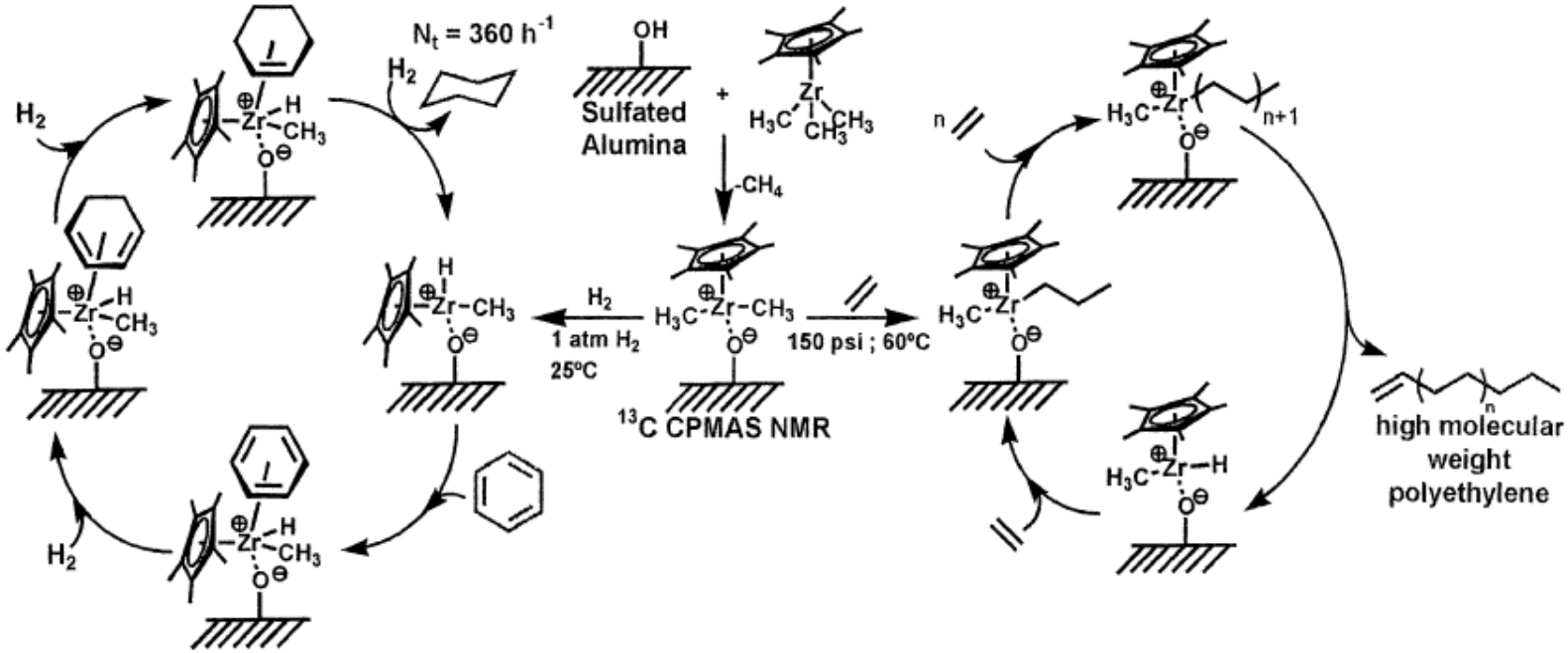

Fig. 2 Metallocene catalysts, used widely in homogeneous solution and typified by zirconcene, are also very efficient in hydrogenations and polymerizations when anchored as single sites on acidic alumina surfaces. (Taken, with kind permission from the work of TJ Marks, Northwestern University)

Solid State Aspects: Going underneath the surface and beyond the molecule

ANGEWANDTE CHEMIE

HERAUSGEGEBEN VON DER GESELLSCHAFT DEUTSCHER CHEMIKER

67. Jahrgang · Nr. 17/18 · Seite 433–540 · 7. September 1955

FORTSETZUNG DER ZEITSCHRIFT »DIE CHEMIE«

Neuere Gedanken zur Natur der heterogenen Katalyse

Von Prof. Dr. GEORG-MARIA SCHWAB[1])

Physikalisch-Chemisches Institut der Universität München

In letzter Zeit sind nähere Aufschlüsse über die Natur der Grenzflächenkatalyse durch die Anwendung der Festkörperphysik erreicht worden. Versuche an Legierungen haben gezeigt, daß die Aktivierung in einem Übergang von Elektronen entweder zum oder vom Katalysator besteht. Inzwischen haben diese Gesichtspunkte sich auch auf halbleitende Oxydkatalysatoren übertragen lassen. Die Chemisorption ist somit als Elektronenübergang deutbar. Verschiedene neuere Einzelfälle werden beschrieben.

Dehydrogenation of formic acid with different bronze alloys: **activation energy** and **resistivity**

$$HCOOH \rightarrow CO_2 + H_2$$

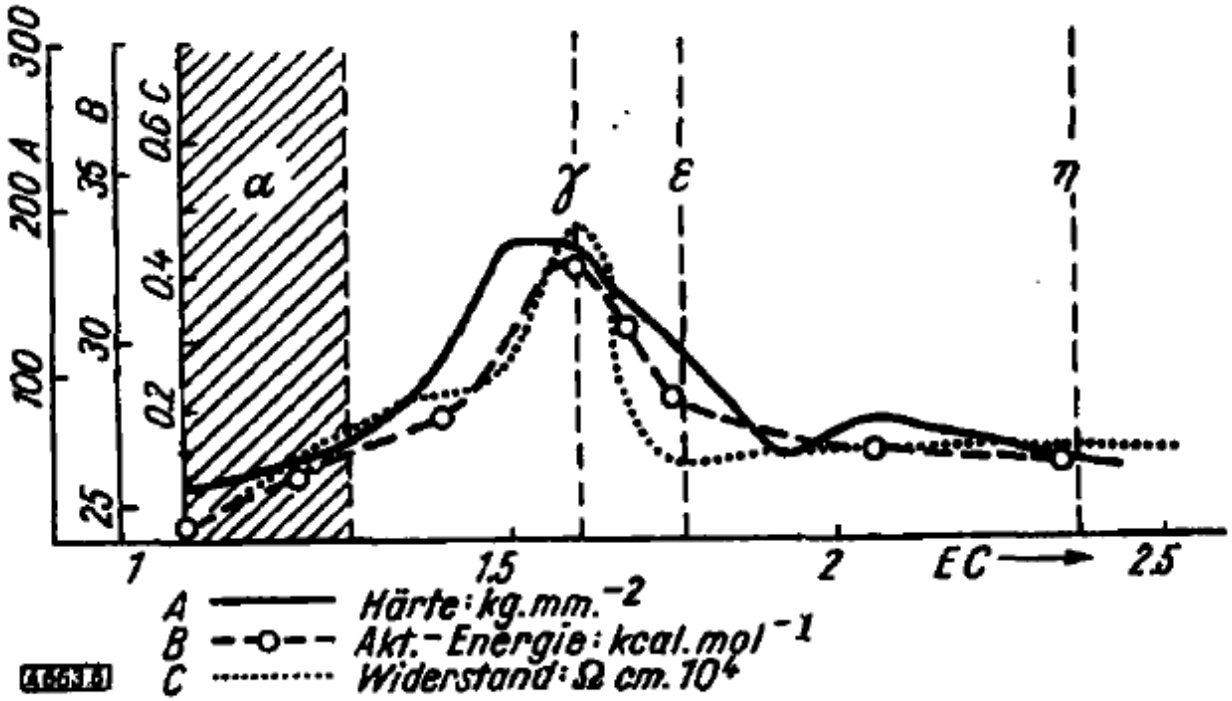

Bild 6

Aktivierungsenergie, Widerstand und Härte bei Bronzen verschiedener Elektronenkonzentration EC

Defect electrons (holes) in NiO (with O excess): **p-type semiconductor**

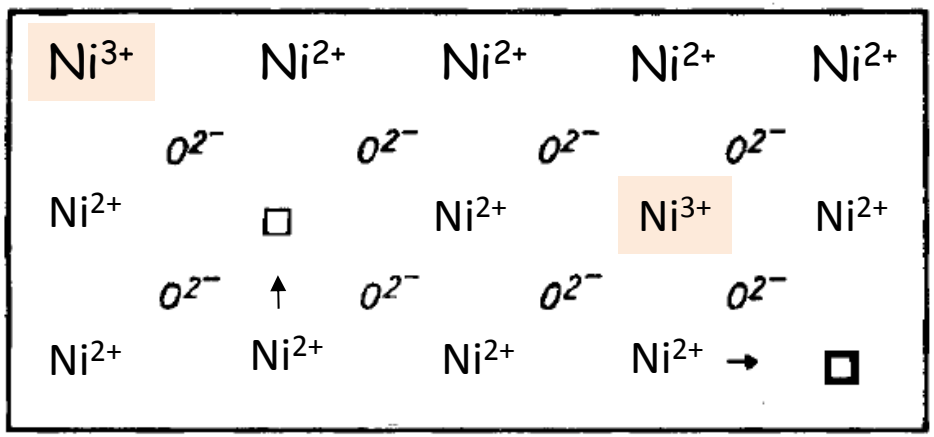

Explanation: donor reaction

defect electron + Ni^{2+} = active site

$$CO + Ni^{3+} \rightarrow (CO^{+})_{ads} + Ni^{2+}$$

$$(CO^{+})_{ads} + Ni^{2+} + {}^{1}/_{2}\,O_2 \xrightarrow{\text{fast}} CO_2 + Ni^{3+}$$

→ *CO chemisorption rate-determining*

Increase of defect electrons by Li_2O, decrease by Cr_2O_3 addition:
$CO + \frac{1}{2}O_2 \rightarrow CO_2$

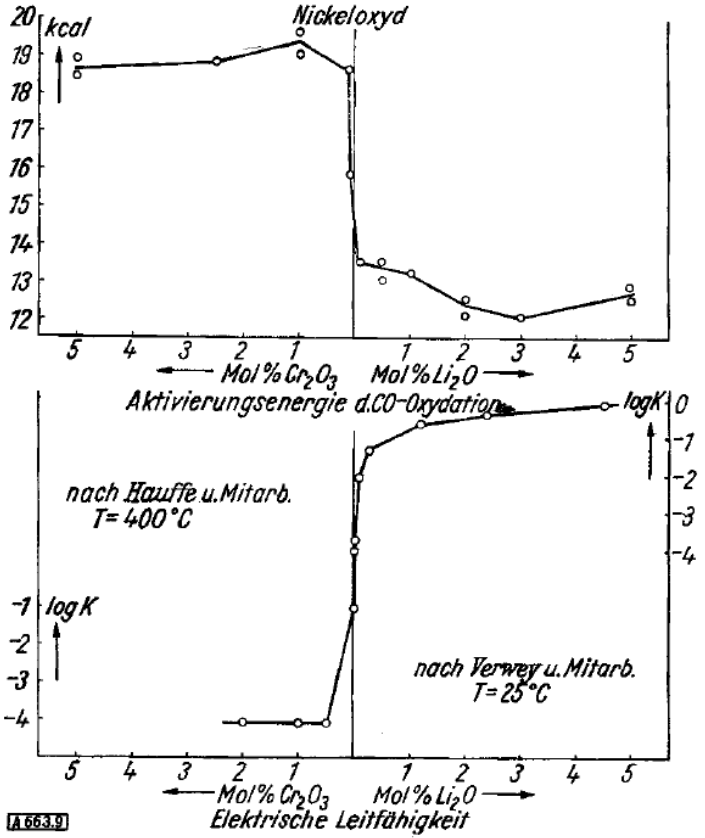

Bild 9
Leitfähigkeit und Aktivierungsenergie an dotiertem NiO

Excess electrons in ZnO (with Zn excess): **n-type semiconductor**

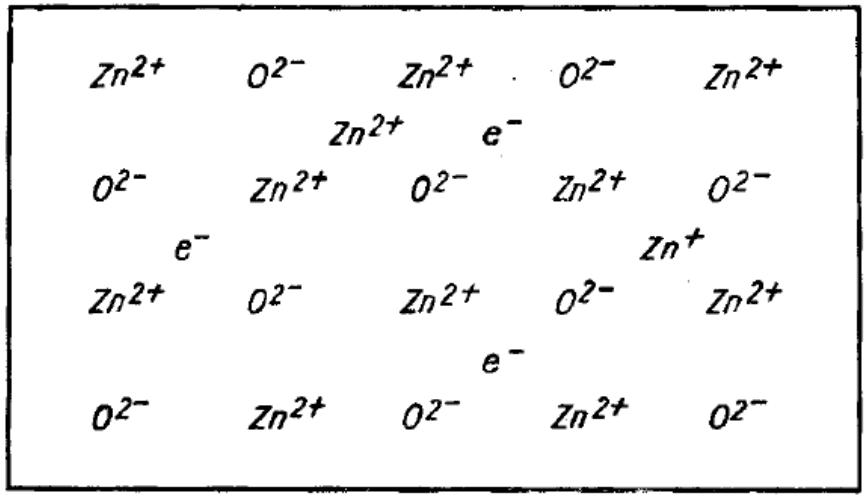

Explanation: acceptor reaction

Zn^{2+} + (1 or 2) quasi-free electrons = active site

$$Zn + {}^1/_2\, O_2 \rightleftharpoons ZnO\,,$$

fast

$$ZnO + CO \rightarrow Zn + CO_2$$

→ *Oxidation of active site rate-determing (strong influence of oxygen on rate)*

Increase of quasi-free electrons by Ga_2O_3, decrease by Li_2O addition:
$CO + \frac{1}{2}O_2 \rightarrow CO_2$

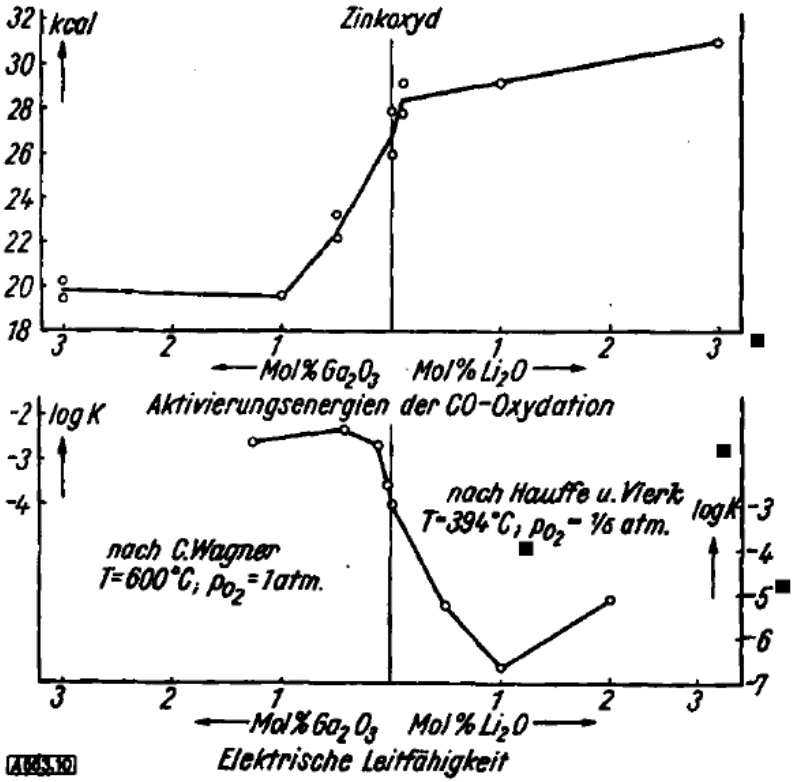

Bild 10

Leitfähigkeit und Aktivierungsenergie an dotiertem ZnO

Kröger-Vink notation for point defects in crystals

F. A. Kröger, H. J. Vink, *Solid State Phys.* **1956**, *3*, 307

Precise description of point defects possible; differentiation between bulk vacancies, interstitials, surface vacancies, adsorbed ions etc.

Symbol	Type of defect
V_M''	Metal ion vacancy: vacant metal site with effective charge −2 (with respect to the ideal lattice)
$V_X^{\bullet\bullet}$	X ion vacancy: vacant X site with effective charge +2 (with respect to the ideal lattice)
M_M^x, X_X^x	Metal, respectively, X ion on their normal lattice position (neutral)
L_M'	L^+ dopant ion on metal site with effective charge −1 (with respect to the ideal lattice)
$N_M^{\bullet}$	N^{3+} dopant ion on metal site with effective charge +1 (with respect to the ideal lattice)
e'	(Quasi)-free electron in conduction band
$h^{\bullet}$	(Quasi)-free electron hole in valence band
$M_i^{\bullet\bullet}$	Interstitial metal ion with effective charge +2 (with respect to the ideal lattice)
X_i''	Interstitial X ion with effective charge −2 (with respect to the ideal lattice)
M_M'	Monovalent metal ion on M^{2+}-position (localised electron, only possible if the metal M has multiple valencies)
$M_M^{\bullet}$	Trivalent metal ion on M^{2+}-position (localised electron hole, only possible if the metal M has multiple valencies)

P. J. Gellings, H. J. M. Bouwmeester, *Catal. Today* **2000**, *58*, 1

Examples: Ni^{3+} in $Ni^{2+}O^{2-}$ on normal lattice position → $Ni_{Ni}^{\bullet}$

Interstitial Zn^{+} in $Zn^{2+}O^{2-}$ → $Zn_i^{\bullet}$

2. Electrical Conductivity in Solid Oxides

1) Proton conduction in oxides

2) Oxygen conduction in oxides

Formation of protonic defects:

Doubly ionized oxygen vacancy

1) Reaction with water $O_O^x + V_O^{\bullet\bullet} + H_2O(g) \rightarrow 2OH_O^{\bullet}$

„normal" lattice oxygen hydroxyl group on regular oxygen position

J. Phys. Chem. C **2010**, *114*, 3609–3613

Water Effect on the Electronic Structure of Active Sites of Supported Vanadium Oxide Catalyst $VO_x/TiO_2(001)$

Oxygen vacancy

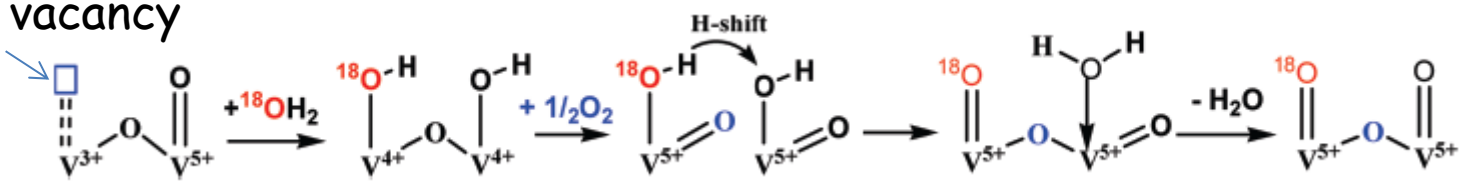

2) Reaction with hydrogen and electron holes

$$2h^{\bullet} + 2O_O^x + H_2 \rightarrow 2OH_O^{\bullet}$$

3) Reaction with hydrogen and formation of free electrons

$$2O_O^x + H_2 \rightarrow 2OH_O^{\bullet} + 2e'$$

Proton conduction mechanisms:

1) Proton hopping (Grotthus mechanism): proton hops between adjacent oxygen ions (large H^+/D^+ isotope effect)

$$OH^- + O^{2-} \rightarrow [O \cdots H \cdots O]^{3-} \rightarrow O^{2-} + OH^-$$

2) Hydroxyl-ion migration (vehicle mechanism): negligible H^+/D^+ isotope effect

Example: Oxidation of propene to acrylic acid on $MoVTeNbO_x$ (M2)

Catalysis Today 155 (2010) 311–318

Contents lists available at ScienceDirect

Catalysis Today

journal homepage: www.elsevier.com/locate/cattod

Electrical conductivity of a MoVTeNbO catalyst in propene oxidation measured in operando conditions

M. Caldararu [a,*], M. Scurtu [a], C. Hornoiu [a], C. Munteanu [a], T. Blasco [b,**], J.M. López Nieto [b]

[a] *Institute of Physical Chemistry "Ilie Murgulescu" of the Romanian Academy, Spl. Independentei 202, 060021 Bucharest, Romania*
[b] *Instituto de Tecnología Química, UPV-CSIC, Campus Universidad Politécnica de Valencia, Avda. Los Naranjos s/n, 46022 Valencia, Spain*

2. Electrical Conductivity in Solid Oxides

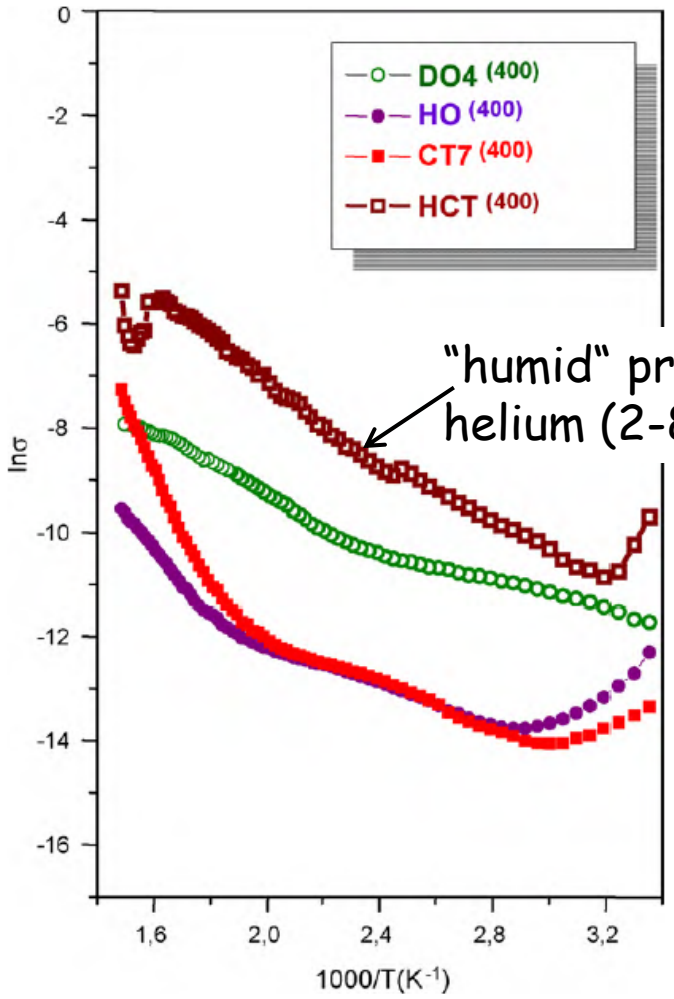

"humid" propene-oxygen-helium (2-8-90) mixture

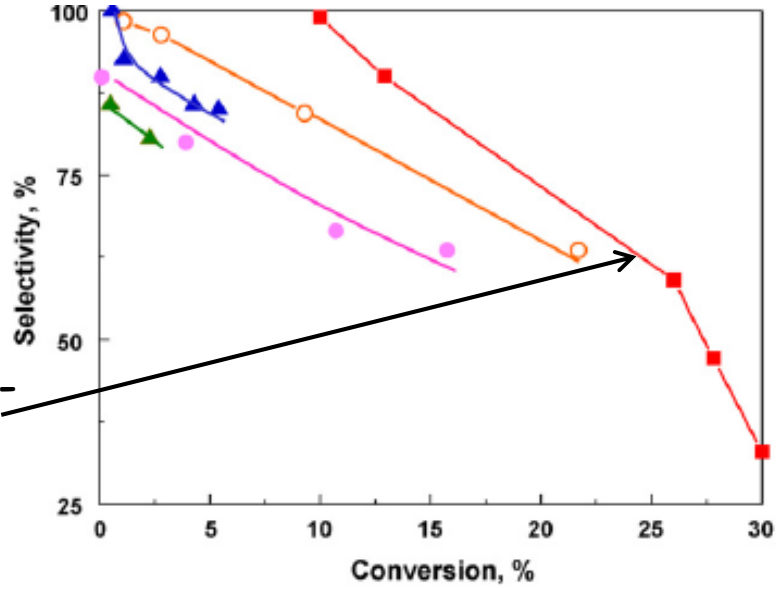

Fig. 7. Variation of selectivity to acrylic acid with propene conversion during various testing cycles: $CT5^{(350)}$ (●); $CT6^{(400)}$ (▲); $CT7^{(400)}$ (○); $HCT^{(400)}$ (■). For comparison, the selectivity achieved at 300 °C during the $CT4^{(300)}$ experiment is also included (▲). (For interpretation of the references to color in this figure legend, the reader is referred to the web version of the article.)

The presence of moisture in the hydrocarbon–oxygen mixture fed on the pre-reduced oxide increases the surface conductivity. This can be tentatively explained by assuming that the anion vacancies are partly filled with adsorbed water instead of oxygen during the low (room) temperature flushing sequence. Part of these water species desorbs on heating, and another part is chemisorbed on further heating, inhibiting extensive surface oxidation.

1) Proton conduction in oxides

2) Oxygen conduction in oxides

Oxygen conduction or How is oxygen incorporated into oxides?

Existing point defects (oxygen vacancies: $V_O^{\cdot\cdot}$, oxygen interstitials: $O_i^{''}$, electronic point defects: $h^{\cdot}$, e') allow a finite compositional flexibility in a binary oxide MO with phase width $MO_{1-\delta}$

$$\Delta\delta/2\,O_2 + MO_{1-\delta} \rightleftharpoons MO_{1-\delta+\Delta\delta}$$

Example: Fe-doped $SrTiO_{3-\delta}$ (quasi-binary due to fixed Sr/Ti ratio below 1200°C)

Table 1: Defect equilibria [Eqs. (2)–(7)] for Fe-doped $SrTiO_{3-\delta}$.

	Reaction[a]		Mass-action law
oxygen incorporation:	$1/2\,O_2 + V_O^{\bullet\bullet} \rightleftharpoons O_O^{\times} + 2h^{\bullet}$	(2)	$K_{ox} = \frac{[h^{\bullet}]^2}{\sqrt{pO_2}[V_O^{\bullet\bullet}]}$
$Fe^{3+/4+}$ redox reaction:	$Fe_{Ti}^{\times} \rightleftharpoons Fe_{Ti}' + h^{\bullet}$	(3)	$K_{Fe} = \frac{[Fe_{Ti}'][h^{\bullet}]}{[Fe_{Ti}^{\times}]}$
band-gap excitation:	$0 \rightleftharpoons e' + h^{\bullet}$	(4)	$K_{bg} = [e'][h^{\bullet}]$
	Conservation conditions:		
iron mass balance:	$[Fe]_{tot} = [Fe_{Ti}'] + [Fe_{Ti}^{\times}]$	(5)	
charge neutrality:	$2[V_O^{\bullet\bullet}] + [h^{\bullet}] = [Fe_{Ti}'] + [e']$	(6)	
	$2[V_O^{\bullet\bullet}] \approx [Fe_{Ti}']$	(7)	

R. Merkle, J. Maier, *Angew. Chem. Int. Ed.* 2008, 47, 3874 – 3894

Phase diagram for $MO_{1-\delta}$

oxygen incorporation:

$$1/2\,O_2 + V_O^{\bullet\bullet} \rightleftharpoons O_O^{x} + 2h^{\bullet}$$

$$K_{ox} = \frac{[h^{\bullet}]^2}{\sqrt{pO_2}[V_O^{\bullet\bullet}]}$$

$Fe^{3+/4+}$ redox reaction:

$$Fe_{Ti}^{x} \rightleftharpoons Fe_{Ti}' + h^{\bullet}$$

$$K_{Fe} = \frac{[Fe_{Ti}'][h^{\bullet}]}{[Fe_{Ti}^{x}]}$$

band-gap excitation:

$$0 \rightleftharpoons e' + h^{\bullet}$$

$$K_{bg} = [e'][h^{\bullet}]$$

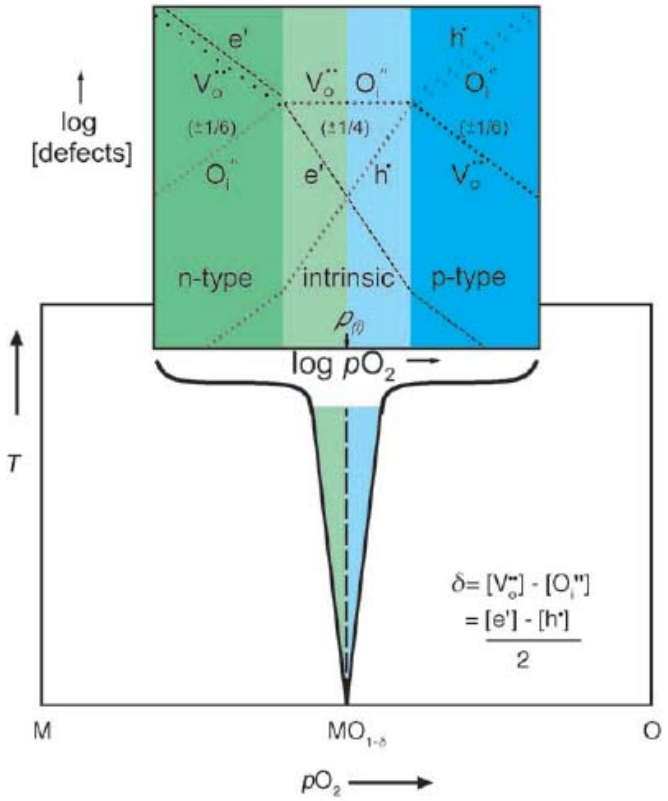

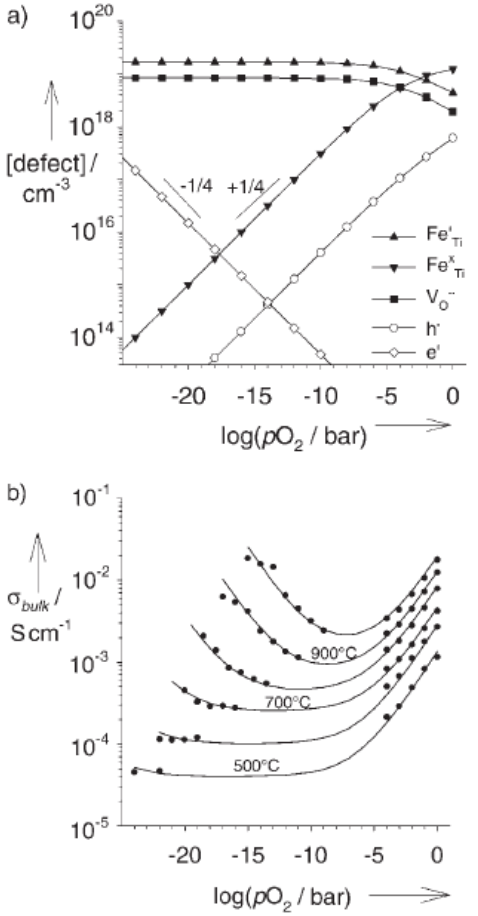

Figure 3. a) Point defect concentrations in Fe-doped (0.1 mol%) $SrTiO_3$ (700 °C) calculated from the defect-chemical model.[78] b) conductivity of a polycrystalline Fe-doped (0.1 mol%) $SrTiO_3$ sam In the pO_2-independent region, the conductivity is predominantly (oxygen vacancies), whereas at very low and high pO_2 n- and p-ty electronic conductivity prevails.

R. Merkle, J. Maier, *Angew. Chem. Int. Ed.* **2008**, *47*, 3874 – 3894

Reaction and transport of oxygen: kinetic limitations

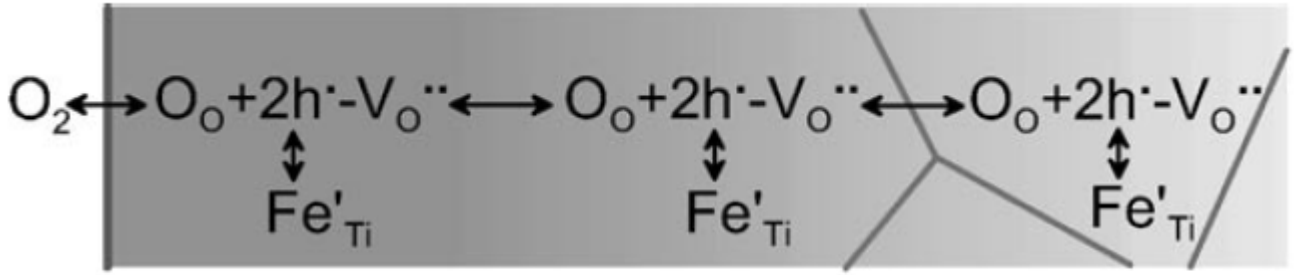

surface reaction $j_O = -\bar{k}^{\delta} \cdot \Delta c_O|_{surf}$

chemical diffusion $j_O = -D^{\delta} \cdot \nabla c_O$

transfer across grain boundary $j_O = -\bar{k}^{\delta}_{gb} \cdot \Delta c_O|_{gb}$

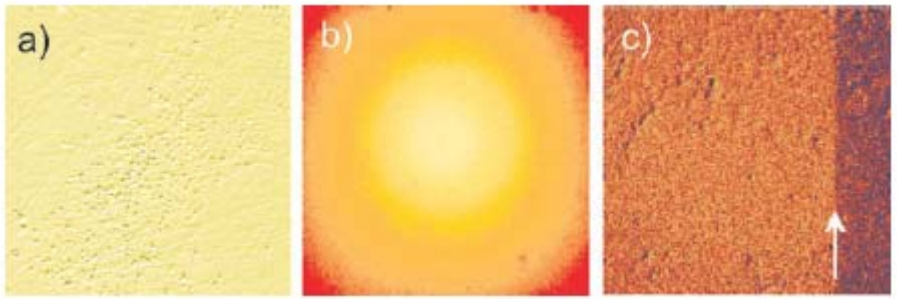

Figure 5. Spatially resolved oxygen concentration after a pO_2 change measured on Fe-doped $SrTiO_3$.[17,18,22,37] $[Fe]_{tot} = 0.3$ mol%, 650°C, sample dimensions 6×6×1 mm. The two large faces are glass sealed so that oxygen can enter only through the small faces. Bright color indicates a high oxygen vacancy concentration. a) single crystal, surface reaction is limiting; b) single crystal, bulk diffusion is limiting; c) 24° [001] symmetrical tilt bicrystal, blocking grain boundary (arrow indicates position of the grain boundary, oxygen diffuses in from the right-hand side).

R. Merkle, J. Maier, *Angew. Chem. Int. Ed.* 2008, 47, 3874 – 3894

2. Electrical Conductivity in Solid Oxides

Fe-doped $SrTiO_3$ single crystal, surface reaction is limiting, T=923 K, pO_2: 0.01->1 bar, t_{total}=24 h

false-color image

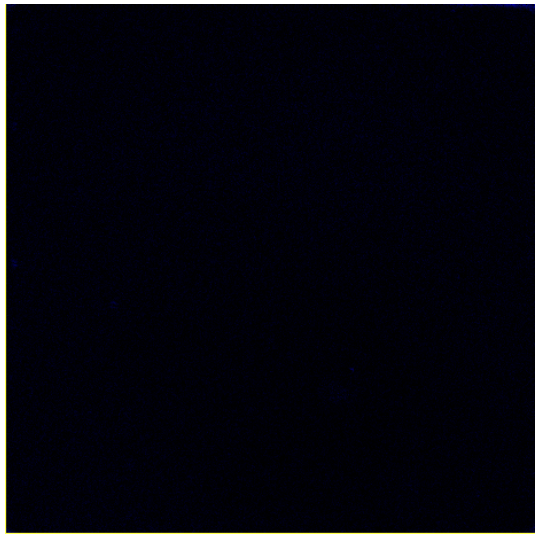

concentration profile

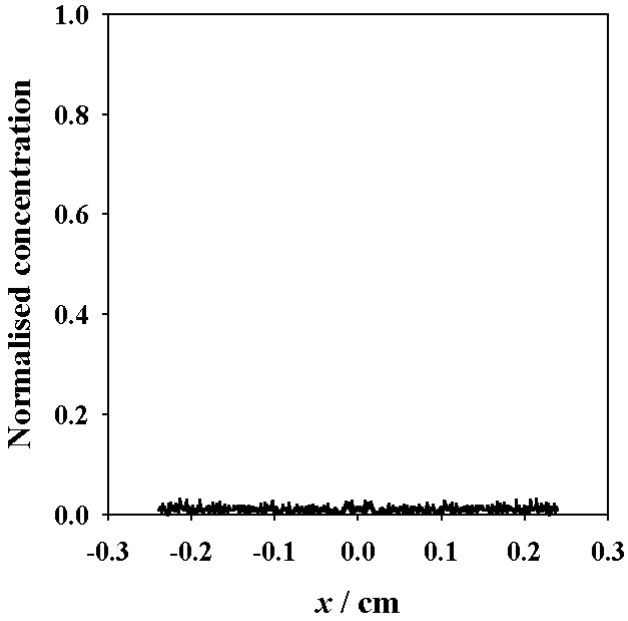

Most probable surface reaction mechanism for Fe-doped $SrTiO_3$:

$$O_2 \rightleftharpoons O_2^- + h^\bullet \quad \text{fast}$$

$$\left.\begin{array}{l} O_2^- + e' \rightleftharpoons O_2^{2-} \\ O_2^{2-} \rightleftharpoons 2O^- \end{array}\right\} \quad \text{rds}^{[a]}$$

$$O^- + V_O^{\bullet\bullet} \rightleftharpoons O_O^{\times} + h^\bullet \quad \text{fast}$$

effective rate constant:

$$\bar{k}^{\delta} = 4\frac{\Re_0}{RT}\frac{\partial \mu_O}{\partial c_O} = 4\Re_0\left(\frac{1}{[V_O^{\bullet\bullet}]} + \chi\frac{4}{[h^\bullet]}\right)$$

exchange rate

$$\Re_0 = \sqrt{\bar{k}\bar{k}[\hat{O}_2^-][\bar{e}'][\hat{O}_2^{2-}]}$$

http://www.fkf.mpg.de/maier/downloads.html

2. Electrical Conductivity in Solid Oxides

Fe-doped $SrTiO_3$ single crystal, bulk diffusion is limiting, T=823 K, pO_2: 0.1->1 bar, t_{total}=6300 s

false-color image

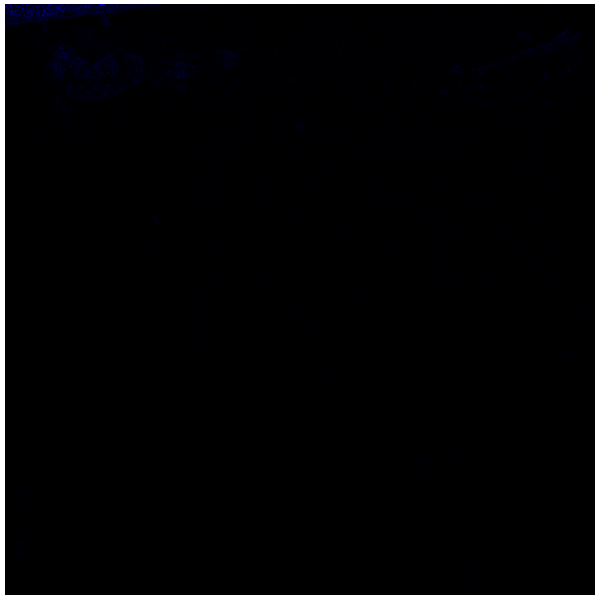

concentration profile

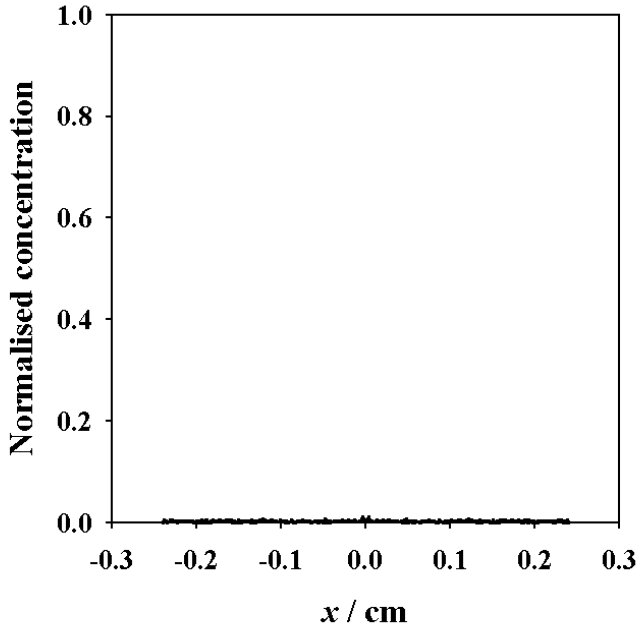

chemical diffusion in the bulk:

(35) $O^{2-}(x) \overset{V_O^{\bullet\bullet}}{\rightleftharpoons} O^{2-}(x')$

(36) $2e^-(x) \overset{2\,h^\bullet}{\rightleftharpoons} 2e^-(x')$

coupled by electroneutrality

$O(x) \rightleftharpoons O(x')$

(37) $-2Fe^{4+} \downarrow\uparrow +2Fe^{4+}$ $\quad\downarrow\uparrow$

$2Fe^{3+}(x) \quad 2Fe^{3+}(x')$

internal reaction reaction "trapping"

chemical diffusion coefficient:

$$D^\delta = \frac{\sigma^\delta}{4F^2}\frac{\partial \mu_O}{\partial c_O} = \frac{RT\sigma^\delta}{4F^2}\left(\frac{1}{[V_O^{\bullet\bullet}]} + \chi\frac{4}{[h^\bullet]}\right)$$

$$\sigma^\delta = \frac{\sigma_{ion}\sigma_{eon}}{\sigma_{ion}+\sigma_{eon}}$$

http://www.fkf.mpg.de/maier/downloads.html

2. Electrical Conductivity in Solid Oxides

Fe-doped $SrTiO_3$ bicrystal, blocking grain boundary, T=873 K, pO_2: 0.1->1 bar, t_{total}=24 h
7.5° tilt grain boundary

false-color image

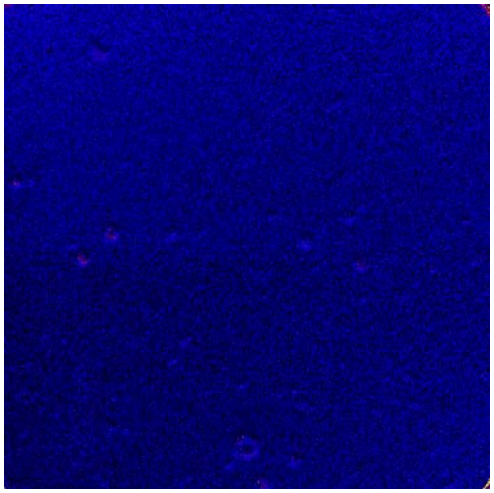

concentration profile

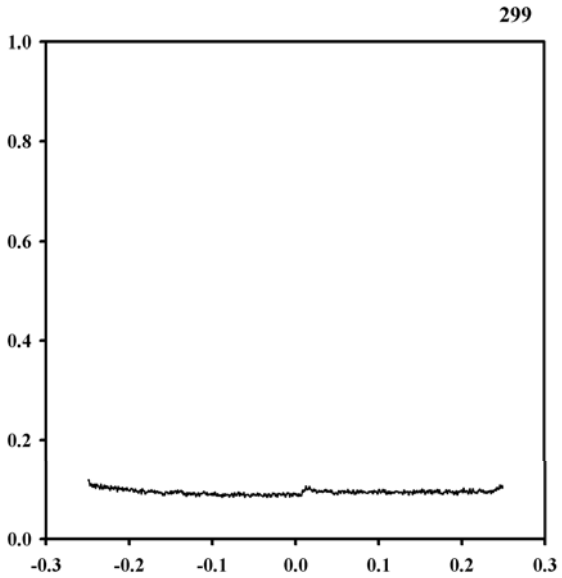

HRTEM image, structural model

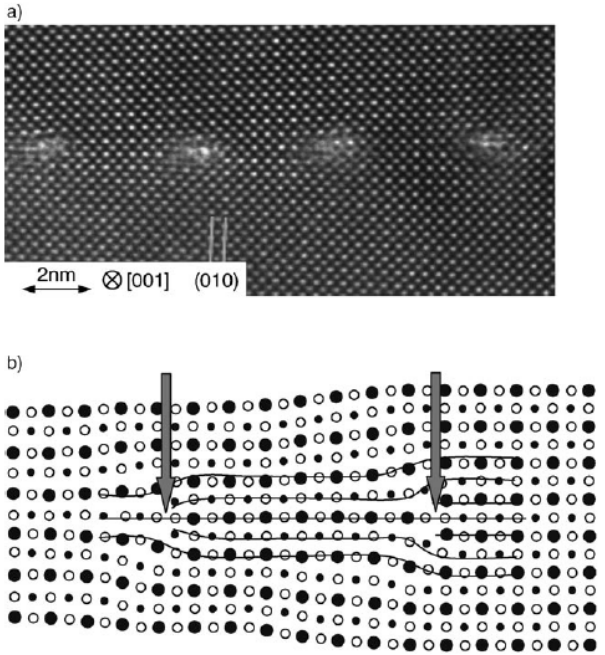

http://www.fkf.mpg.de/maier/downloads.html

Blocking grain boundary → formation of space charge layers

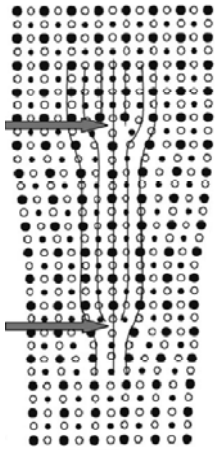

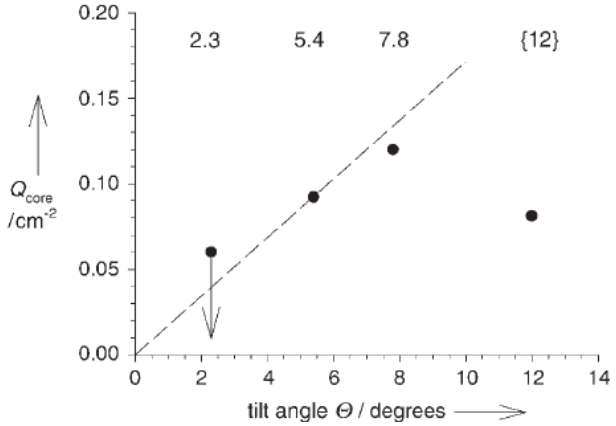

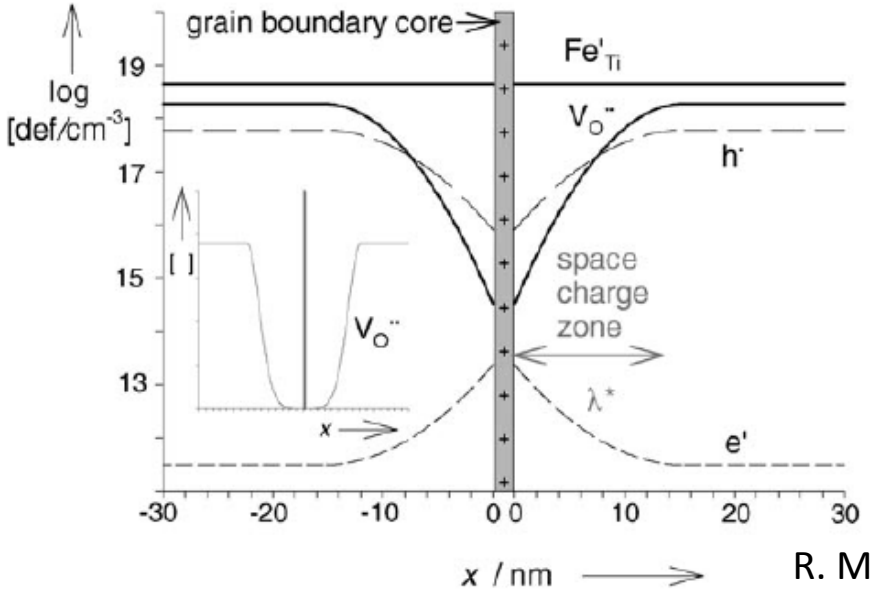

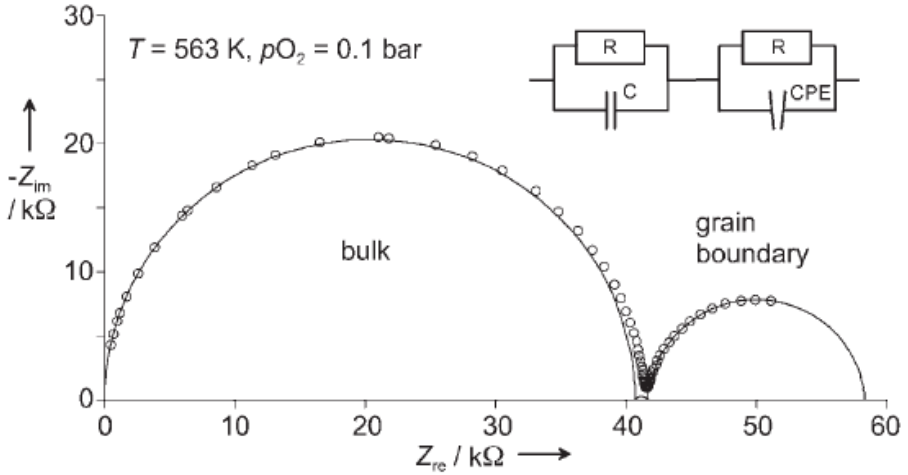

R. Merkle, J. Maier, *Angew. Chem. Int. Ed.* 2008, 47, 3874 – 3894

Localized Impedance Spectroscopy

array of circular gold *microelectrodes* (20 μm diameter) on polycrystalline Fe-doped $SrTiO_3$

platinum contact tips

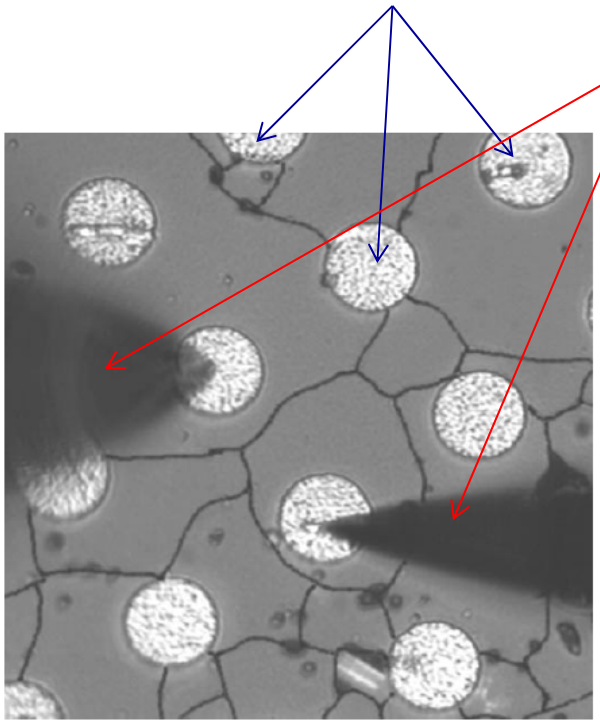

R. Merkle, J. Maier, *Angew. Chem. Int. Ed.* 2008, 47, 3874 – 3894

Insertion: Impedance spectroscopy

Impedance measurements (measurement at alternating voltages):

$$\boldsymbol{U}(t) = \hat{\boldsymbol{U}} e^{i(\omega t + \phi_U)}$$

$$\boldsymbol{I}(t) = \hat{\boldsymbol{I}} e^{i(\omega t + \phi_I)}$$

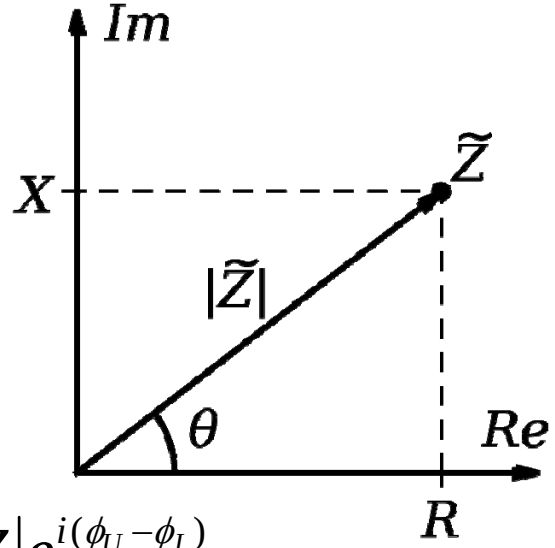

Impedance [Ω]: $|Z| = \frac{\hat{\boldsymbol{U}}}{\hat{\boldsymbol{I}}} = \sqrt{R^2 + X^2}$

Complex impedance: $\boldsymbol{Z} = R + iX = |Z| e^{i\theta} = |Z| e^{i(\phi_U - \phi_I)}$

Resistance, Reactance, Phase difference between voltage and current

Ohm`s law: $\boldsymbol{U} = \boldsymbol{I}\boldsymbol{Z} = \boldsymbol{I}|Z|e^{i\theta}$

Impedance of an ideal resistor: $Z_R = R$

Impedance of an ideal inductor: $Z_L = i\omega L = \omega L e^{i\frac{\pi}{2}}$

Impedance of an ideal capacitor: $Z_C = \frac{1}{i\omega C} = \frac{1}{\omega C} e^{i(-\frac{\pi}{2})}$

Total impedance calculated by using rules for combining impedances in series and parallel:

Series combination: $Z_{tot} = Z_1 + Z_2 + \ldots + Z_n$

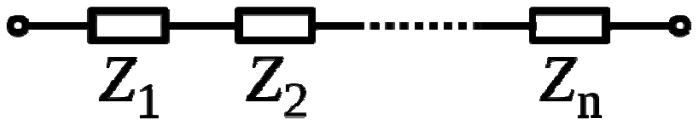

Parallel combination: $1/Z_{tot} = 1/Z_1 + 1/Z_2 + \ldots + 1/Z_n$

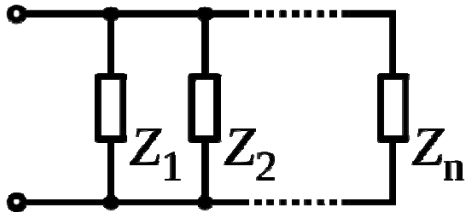

3. Impedance Spectroscopy

Impedance spectroscopy (IE): Sinosoidal voltage, frequency variation (typically between 10^{6} and 10^{-3} Hz)

According to Ohm's law the impedance of a sample can be calculated by complex division of the voltage and current

Looking for an "equivalent circuit" with certain impedance elements that describes best the frequency-dependent behavior of the sample

The impedance elements are related to certain physico-chemical properties, e.g. electrochemical double layer between electrode and electrolyte ions (Helmholtz layer) can be described by a capacitor

Bode plot (phase angle θ vs. frequency)

e.g. oxide layer on Al

one time constant ($\tau = R\,C$)

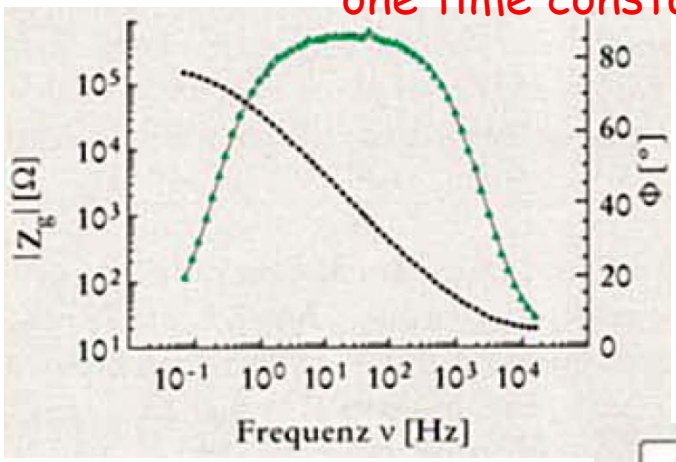

e.g. chromate layer on oxide layer on Al

two time constants

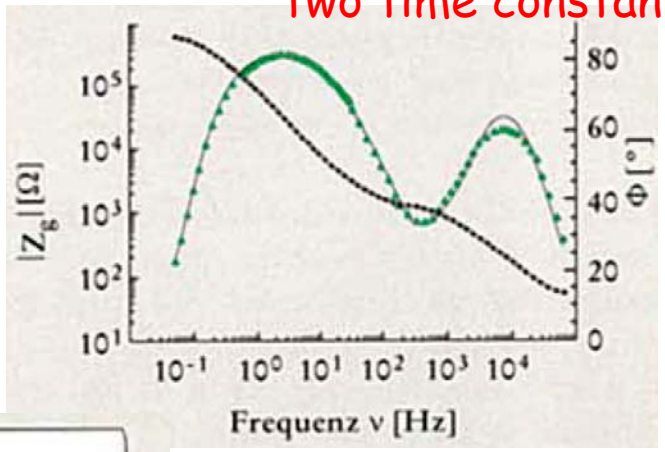

Equivalent circuit:

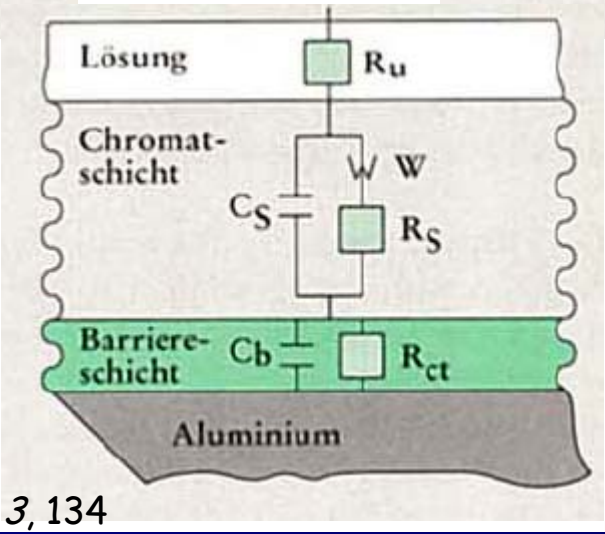

D. Ende, K.-M. Mangold, *ChiuZ* **1993**, *3*, 134

3. Impedance Spectroscopy

Simplified equivalent circuit for a redox reaction:

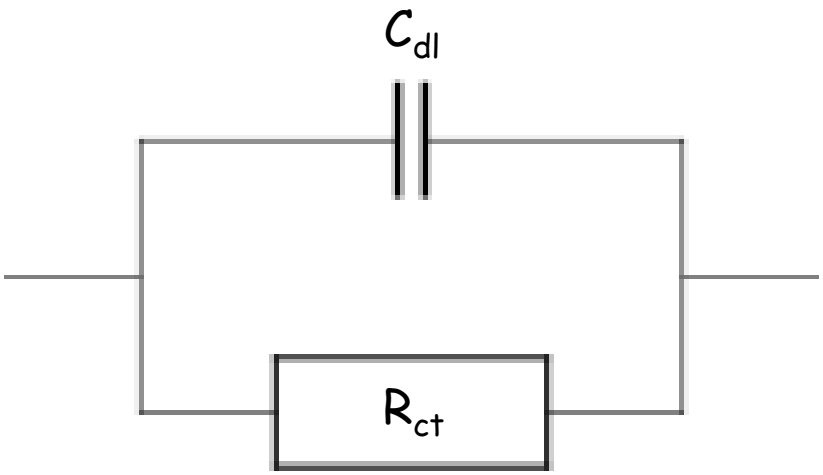

Corresponding Nyquist diagram for RC parallel circuit:

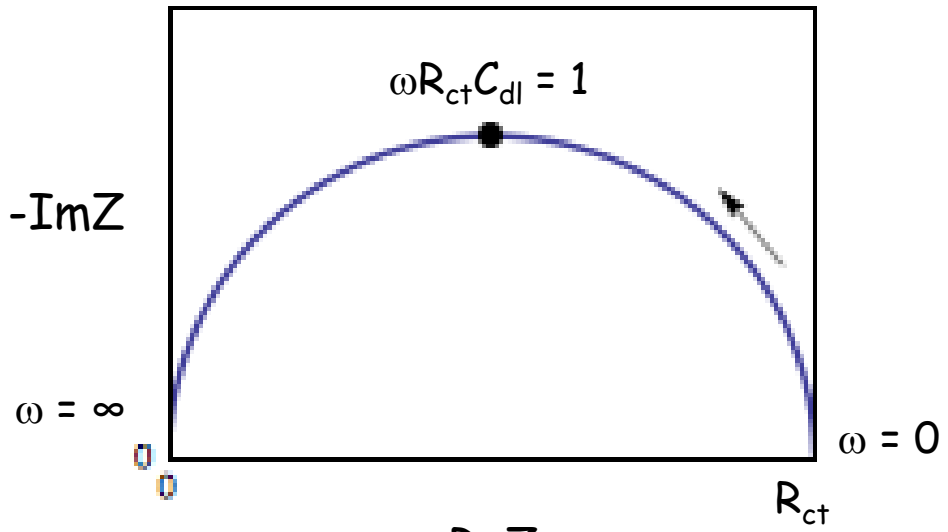

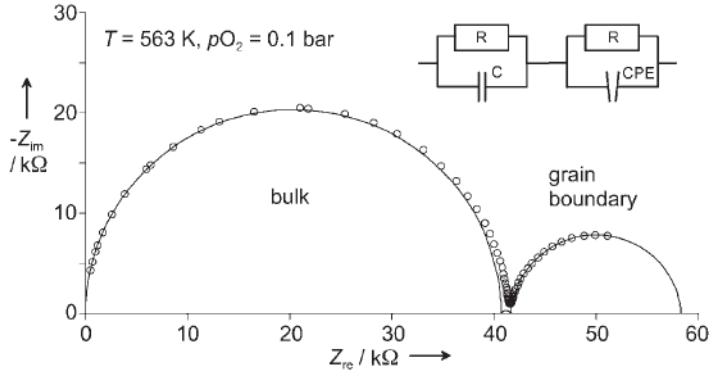

The Physicist's View of a Solid

4. The Physicist`s View of a Solid

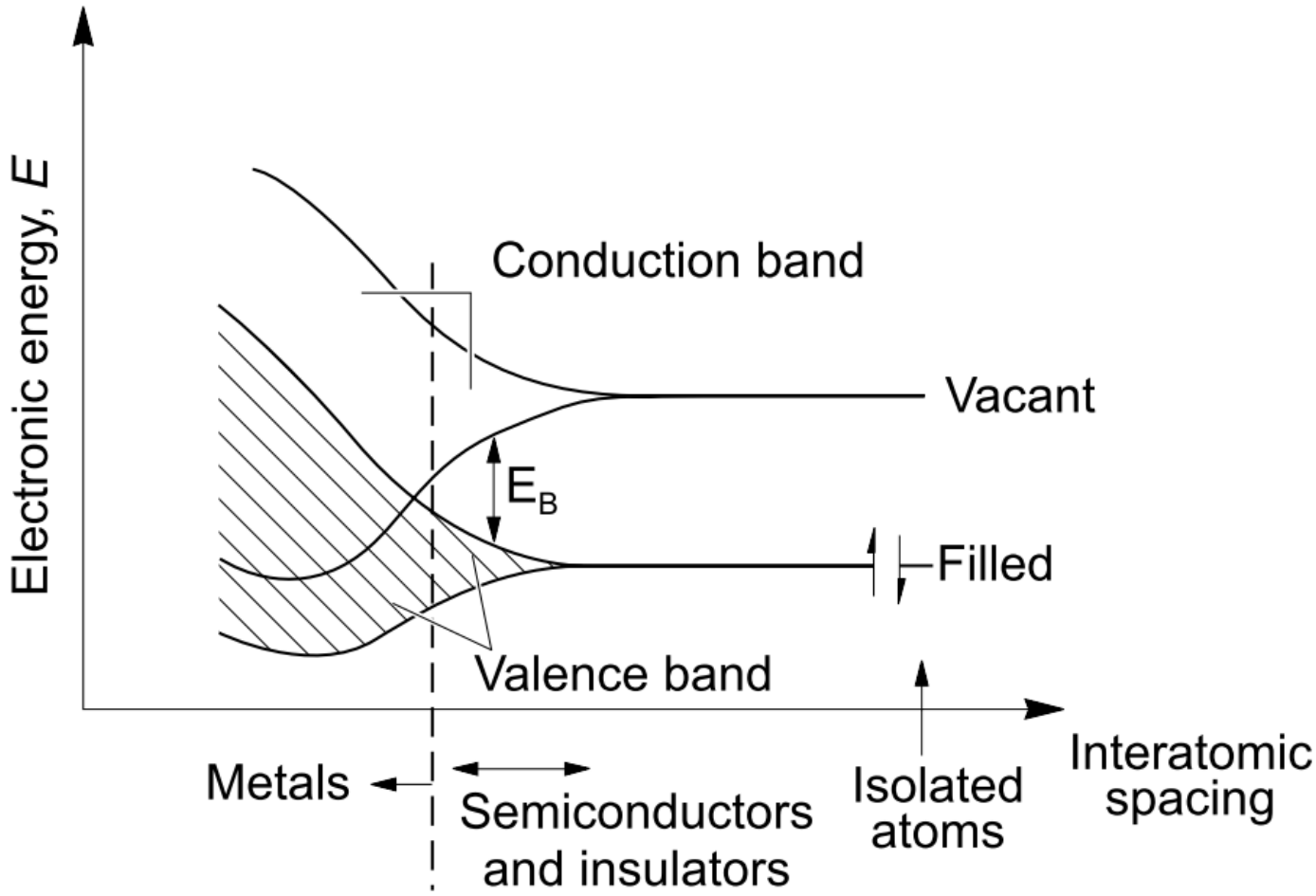

A. W. Bott, *Current Separations* **1998**, *17*, 87

Occupancy of electrons in a band is determined by **Fermi-Dirac statistics**

Fermi-Dirac distribution (for an electron gas):

$$f(E) = \frac{1}{\exp\left(\frac{E-\mu}{k_B T}\right)+1}$$

E...Energy

k_B...Boltzmann constant

T...Temperature

μ...(Electro-)Chemical potential

$$\mu(T=0) = E_{\text{Fermi}}$$

$$f(E=\mu) = 1/2$$

= Fermi level

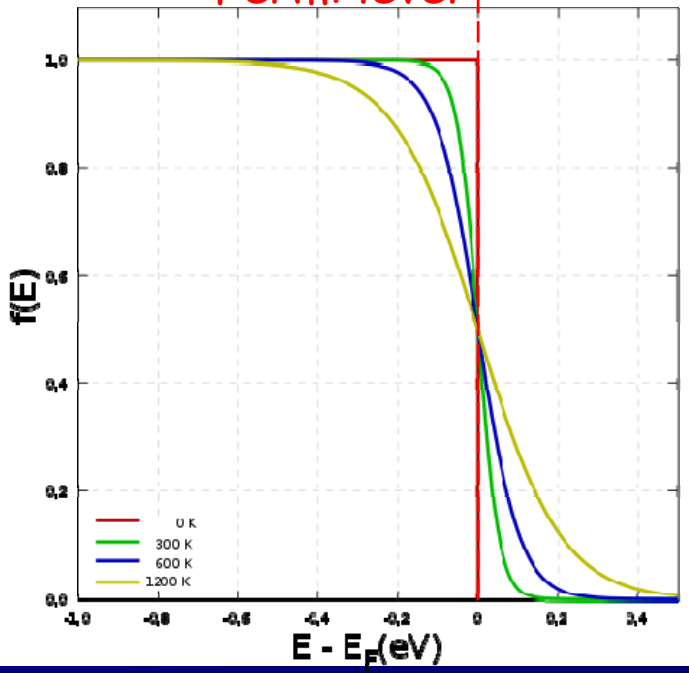

P. A. Tipler, *Physik*, Spektrum Verlag

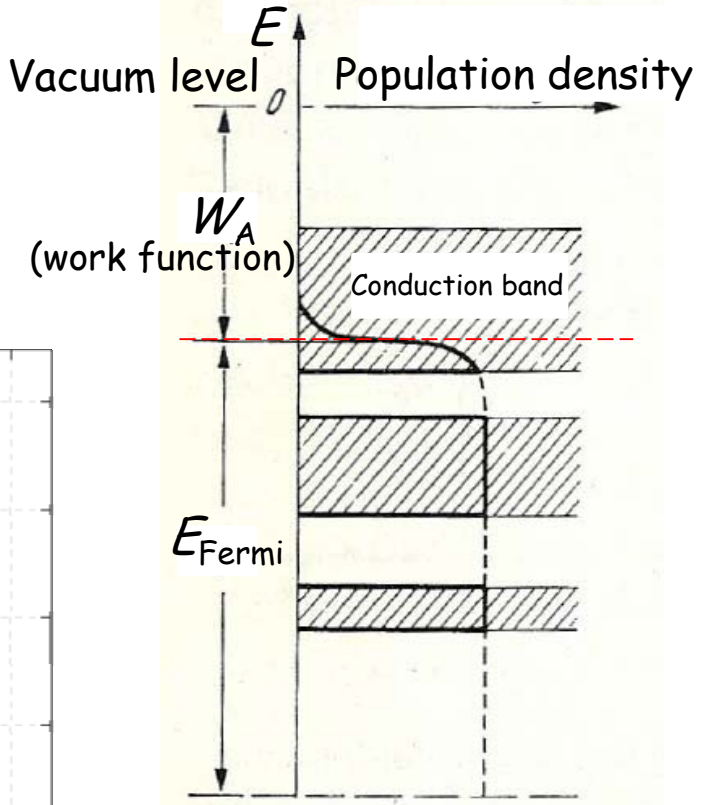

The Fermi curve determines the population of occupied states, independent of the existence of states in the regarded E region

Intrinsic semiconductor

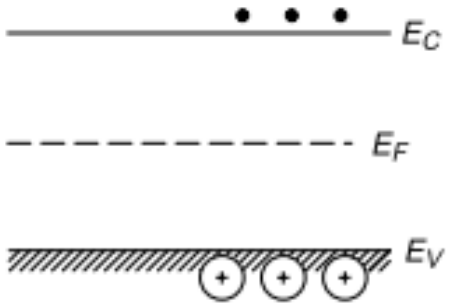

e.g. Si (band gap at 300 K = 1.12 eV)

(Extrinsic) n-type semiconductor

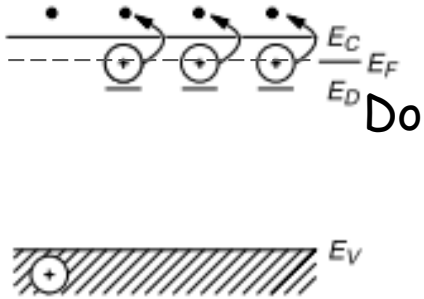

Donor level

e.g. As-doped Si

additional electrons

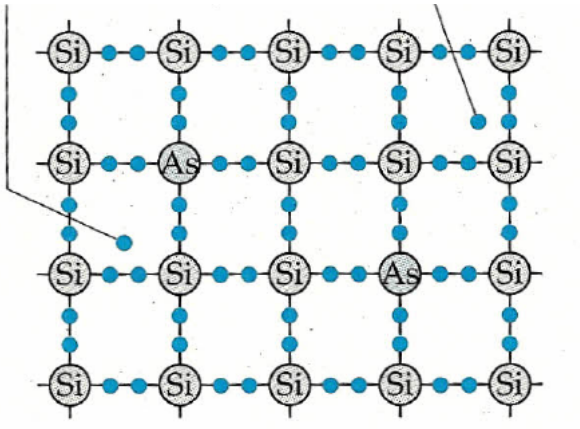

(Extrinsic) p-type semiconductor

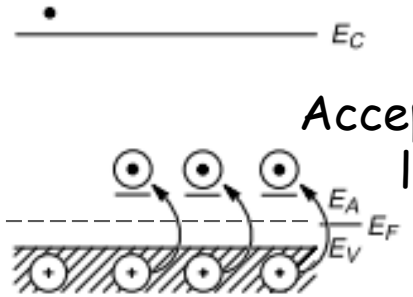

Acceptor level

e.g. Ga-doped Si

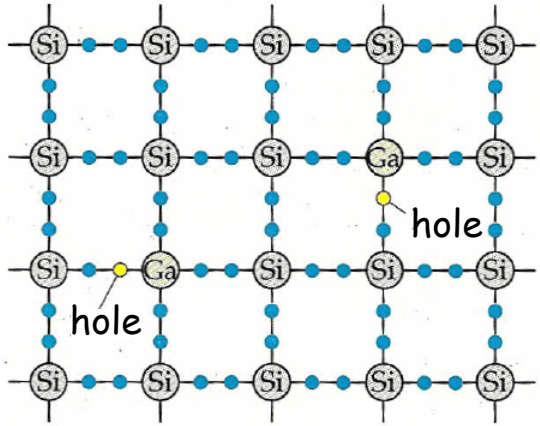

P. A. Tipler, *Physik*, Spektrum Verlag

Space charge region

Metals

Contact voltage = $(W_{A1} - W_{A2})/e$

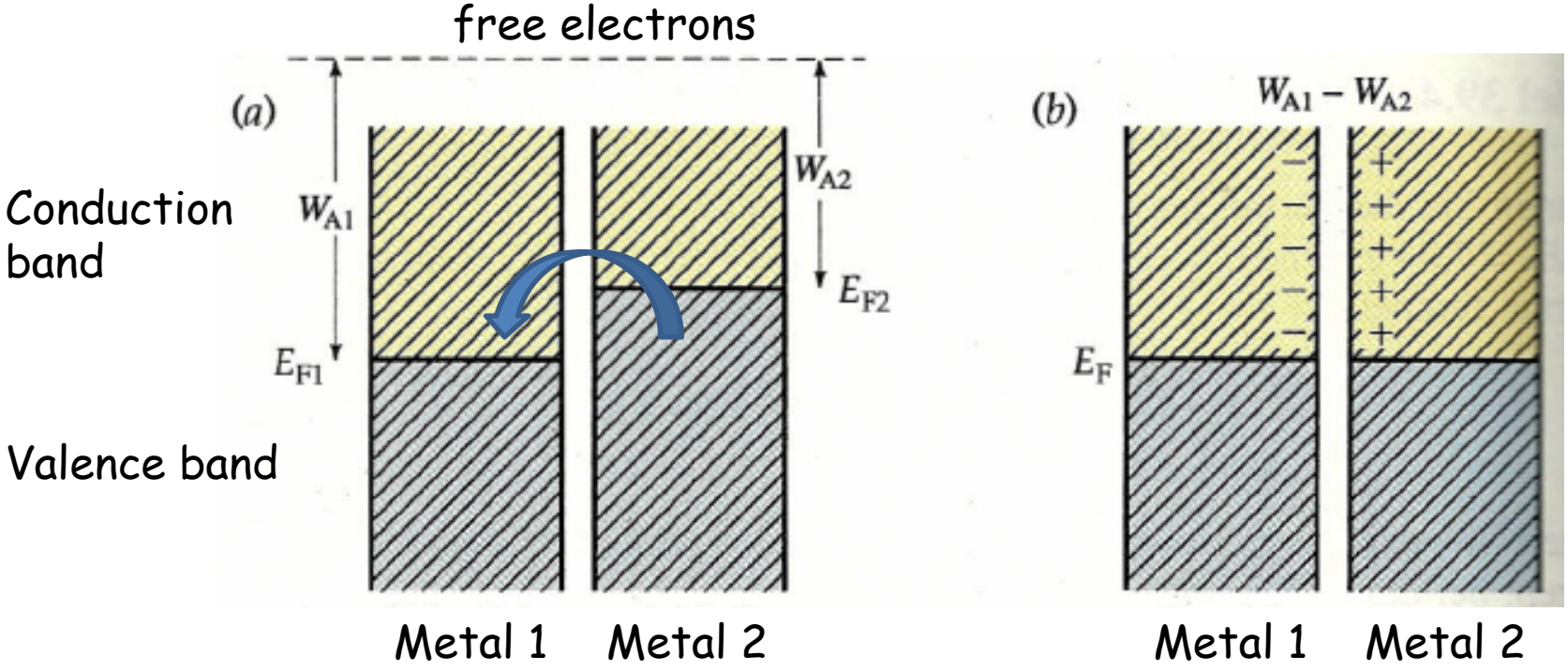

a) Energy states of two different metals with different Fermi energies and work functions. b) With contact, electrons will flow from the metal with higher Fermi energy (lower work function) to the one with lower Fermi energy (larger work function) until the Fermi levels of both metals are equalized

P. A. Tipler, *Physik*, Spektrum Verlag

Semiconductors

n-type SC in contact with electrolyte

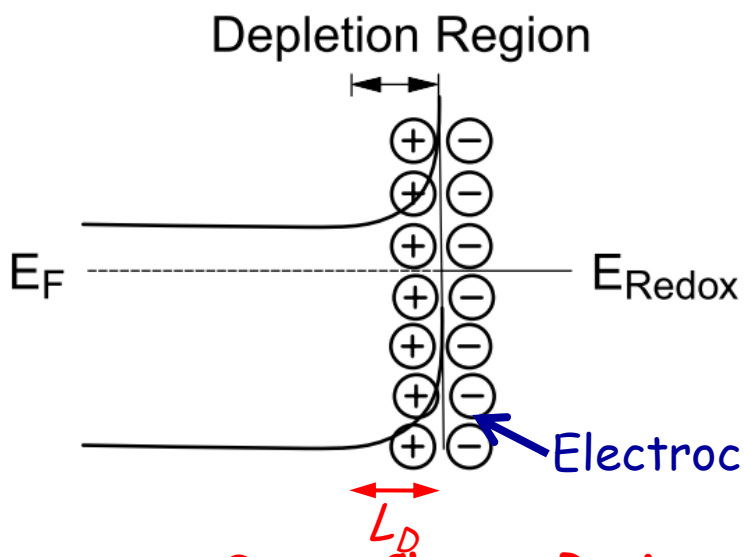

p-type SC in contact with electrolyte

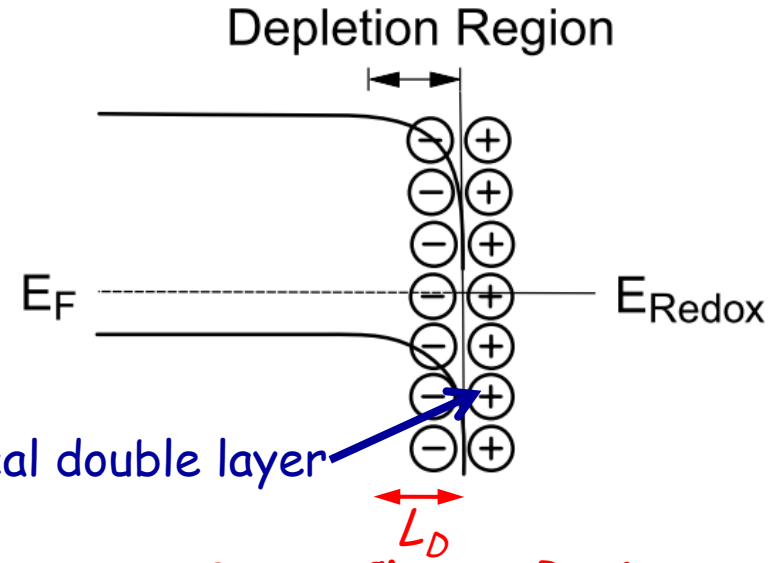

In metals: penetration depth (space charge region to compensate surface charge) of only a few lattice constants (high concentration of free charge carriers)

In SCs: Debye shielding, L_D, can amount from 10 nm to 1 μm

$$L_D = \sqrt{\frac{\varepsilon k_B T}{2\pi q^2 n_i}}$$

ε...Dielectric permittivity of crystal; q...Electron charge; n_i...Concentration of charge carriers in intrinsic semiconductor

A. W. Bott, *Current Separations* **1998**, *17*, 87

External Potential Control

Effect of varying the applied potential (E) on the band edges in the interior of an n-type semiconductor. a) $E > E_{fb}$, b) $E = E_{fb}$, c) $E < E_{fb}$.

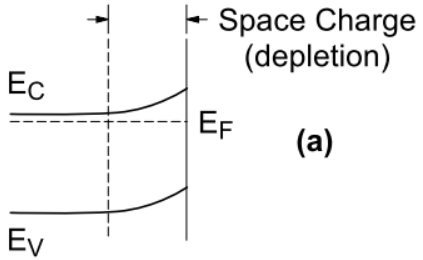

Positive potential

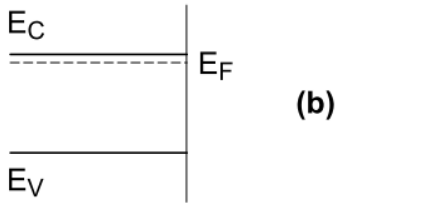

Flatband potential

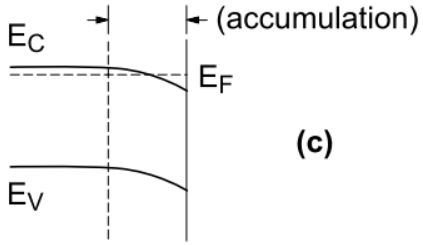

Negative potential

Effect of varying the applied potential (E) on the band edges in the interior of a p-type semiconductor. a) $E > E_{fb}$, b) $E = E_{fb}$, c) $E < E_{fb}$.

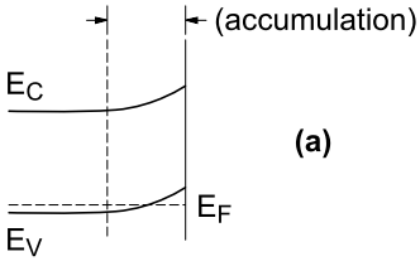

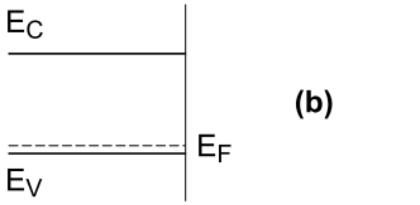

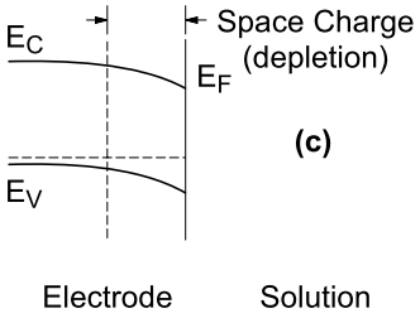

A. W. Bott, *Current Separations* **1998**, *17*, 87

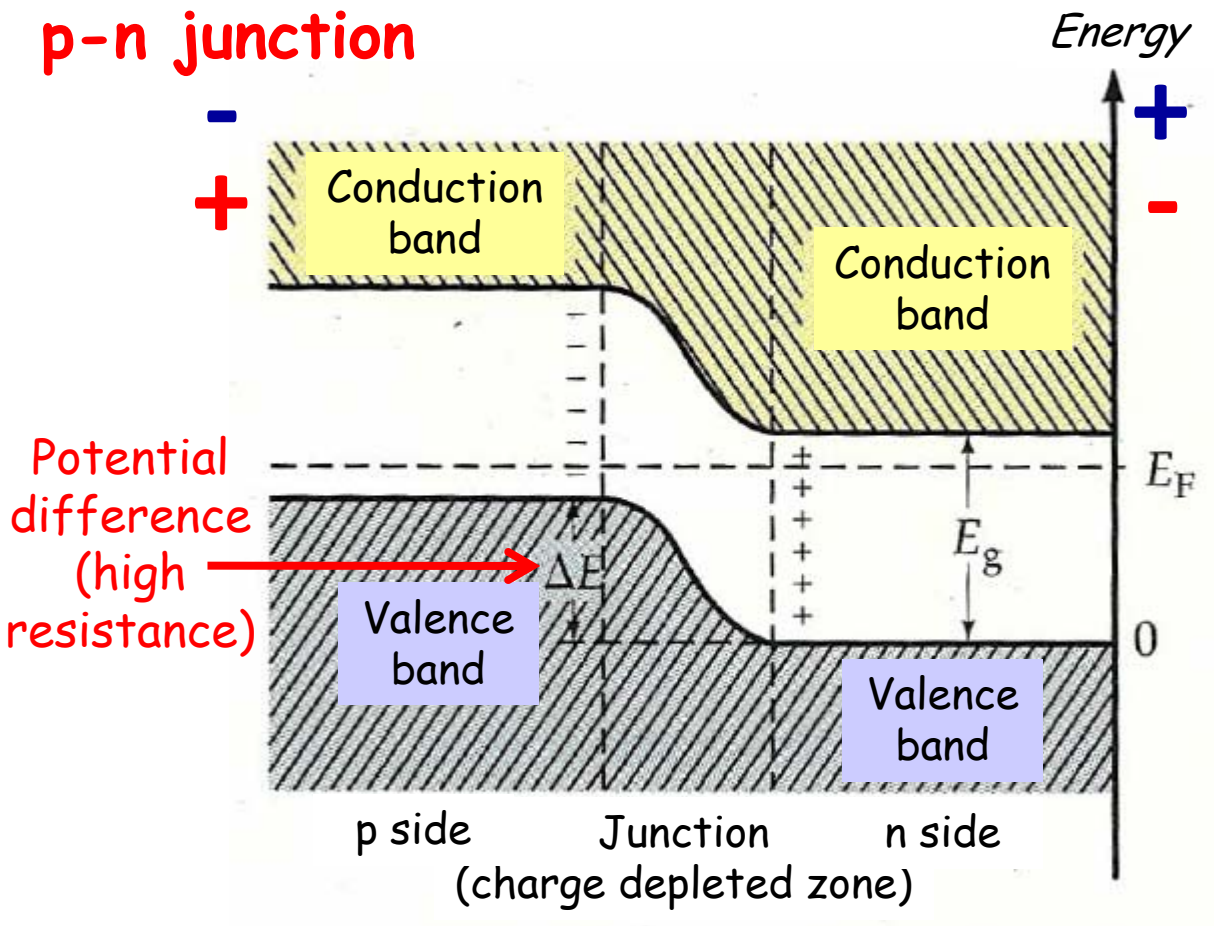

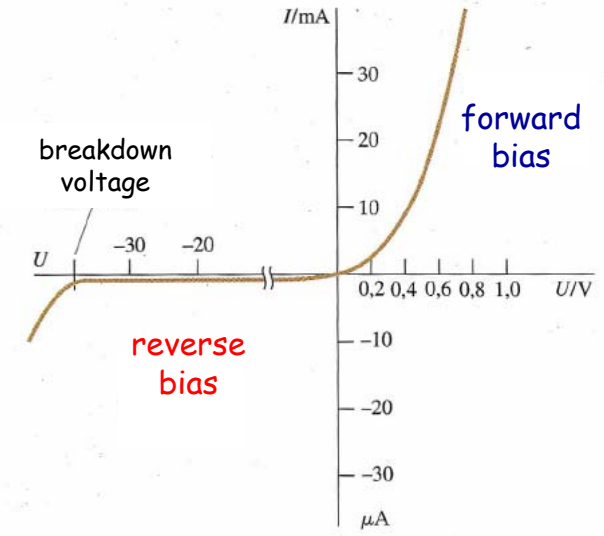

Electrons migrate to p side, holes migrate to n side until electrochemical potentials (Fermi energies) are equilibrated

P. A. Tipler, *Physik*, Spektrum Verlag

Metal-semiconductor junction (Schottky barrier)

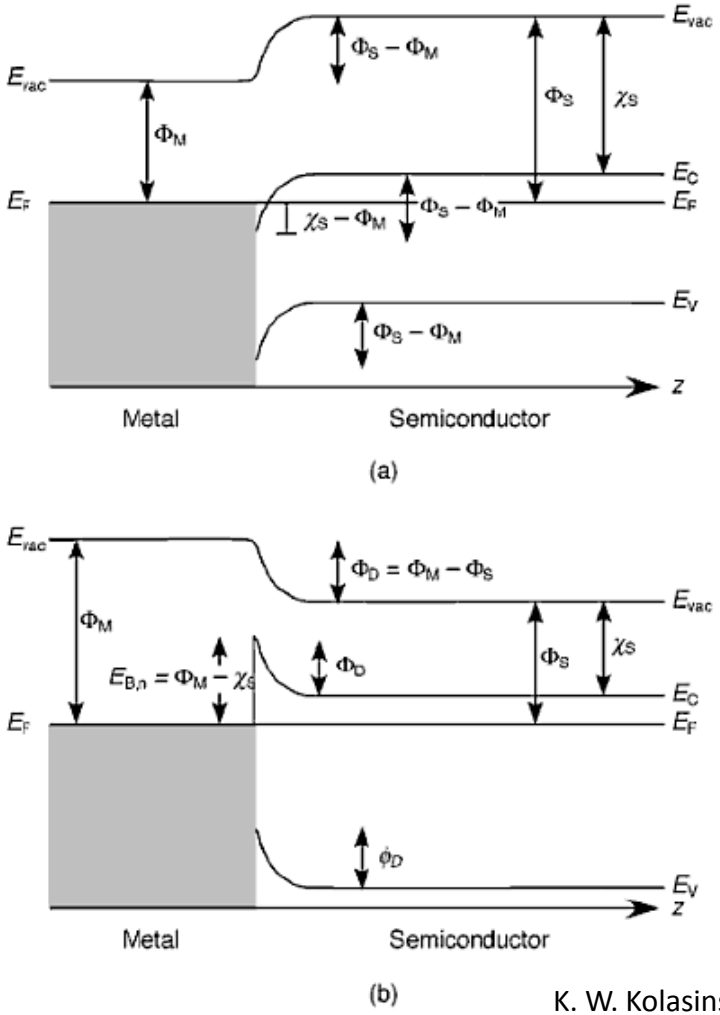

Ohmic contact

Figure 1.17 *Band bending in an n-type semiconductor at a heterojunction with a metal. (a) Ohmic contact ($\Phi_S > \Phi_M$). (b) Blocking contact (Schottky barrier, $\Phi_S < \Phi_M$). The energy of the bands is plotted as a function of distance z in a direction normal to the surface. Φ_S, Φ_M work function of the semiconductor and of the metal, respectively; E_{vac}, vacuum energy; E_C, energy of the conduction band minimum; E_F, Fermi energy; E_V energy of the valence band maximum. Redrawn from S. Elliott, The Physics and Chemistry of Solids. (1998) Copyright, with permission from John Wiley & Sons, Ltd.*

Schottky barrier

K. W. Kolasinski, *Surface Science: Foundations of Catalysis and Nanoscience*, John Wiley & Sons **2008**

Back to Chemistry…

Oxidation catalysis with transition metal ions:

1) Oxidation of the substrate by the catalyst (being reduced)

$$RH + O^{2-} \rightarrow R\text{–}O^{-} + H^{+} + 2e^{-}$$

2) Reoxidation of the catalyst (usually by gas phase oxygen)

$$O_2\,(g) \xrightarrow{V_O^{\cdot\cdot} + e^-}$$

$$\text{adsorbed oxygen } (O_2^-, O_2^{2-}, O^-) \xrightarrow{V_O^{\cdot\cdot} + e^-} O^{2-}\,(s)$$

Experimental hints for the participation of "lattice" oxygen (oxygen covalently bound to the active transition metal ion) in the reaction:

1) Reaction runs (awhile) without gas phase oxygen present (riser reactor concept)

2) Different oxidation states of the transition metal are monitored in dependence on the partial pressures of reaction gases or on contact time

3) By using $^{18}O_2$ in isotope exchange experiments, first ^{16}O (from the catalyst) is found in the reaction product, and only after some time ^{18}O

4) After long $^{18}O/^{16}O$ exchange, ^{18}O is found in the catalyst lattice (e.g. in ToF-SIMS experiments)

5) Conductivity changes upon reaction conditions, correlation between conductivity and activity/selectivity for differently doped semiconductors

Example:

JOURNAL OF CATALYSIS **168,** 315–320 (1997)

The Effect of Oxygen-Anion Conductivity of Metal–Oxide Doped Lanthanum Oxide Catalysts on Hydrocarbon Selectivity in the Oxidative Coupling of Methane

Holger Borchert* and Manfred Baerns†

$$CH_4 + O_x^- \ (x = 1 \text{ or } 2) \Leftrightarrow CH_3^\bullet + HO_x^-$$

$$CH_3\text{–}H + [M^{n+}O^{2-}] \Leftrightarrow [M^{n+}OH^-] + CH_3^- \rightarrow M^{(n-1)+}OH^- + CH_3^\bullet.$$

$$O_2\ (g) \rightleftharpoons O_2\ (s) \overset{e}{\rightleftharpoons} O_2^-\ (s) \overset{e}{\rightleftharpoons} O_2^{2-}\ (s) \rightleftharpoons 2O^-\ (s) \overset{2e}{\rightleftharpoons} 2O^{2-}\ (s)$$

Oxygen-Anion Conductivity σ_{ion} and p-type Conductivity σ_p of La_2O_3 and Me^{n+} (1 at-%)-Doped La_2O_3 Catalysts

Catalyst	$\sigma_{ion}/\Omega^{-1}\,cm^{-1}$	$\sigma_p/\Omega^{-1}\,cm^{-1}$	σ_{ion}/σ_p
Sr^{2+} (1 at-%)/La_2O_3	$2.2 * 10^{-4}$	$2.2 * 10^{-3}$	0.100
Zn^{2+} (1 at-%)/La_2O_3	$8.5 * 10^{-6}$	$1.7 * 10^{-4}$	0.050
La_2O_3	$2.1 * 10^{-6}$	$9.8 * 10^{-5}$	0.021
Nb^{5+} (1 at-%)/La_2O_3	$8.3 * 10^{-7}$	$6.2 * 10^{-5}$	0.013
Ti^{4+} (1 at-%)/La_2O_3	$5.6 * 10^{-7}$	$1.9 * 10^{-5}$	0.029

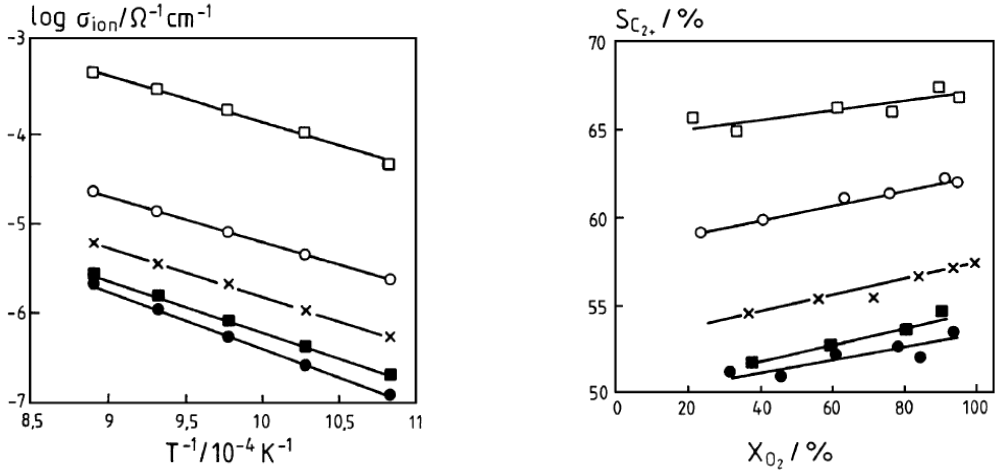

FIG. 1. Arrhenius plot of the dependence of oxygen-anion conductivity on temperature for La_2O_3 and Me^{n+} (1 at-%)/La_2O_3 catalysts. Symbols Me^{n+}: Zn^{2+} (○), Sr^{2+} (□), Ti^{4+} (●), Nb^{5+} (■); La_2O_3 (×).

Participation of "lattice oxygen" is often associated with the Mars-van Krevelen mechanism

Special Suppplement to Chemical Engineering Science, vol. 3. 1954.

Oxidations carried out by means of vanadium oxide catalysts

P. Mars and D. W. van Krevelen

Staatsmijnen in Limburg, Central Laboratory, Geleen, Netherlands

Summary—All technically interesting reactions carried out with vanadium oxide catalysts are marked by their highly exothermic character, which forms an impediment to the investigation of the kinetics of these processes. In the present study use was made of a fluid bed, in which the temperature is uniform. The oxidation of the following substances: benzene, toluene, naphthalene, and anthracene has been studied.

The partial pressures of the reacting substances were varied to the greatest possible extent. Both reaction components appeared to influence the reaction rate. A formula depicting this influence is derived. This formula may be interpreted by assuming two successive reactions, namely the reaction between the aromatic and the oxygen on the surface, and the re-oxidation of the partly reduced surface by means of oxygen.

The formula may be reduced to an equation by which also the data on the oxidation of sulphur dioxide by means of vanadium oxide catalysts found in the literature are well described.

Using kinetic data it is possible to determine the optimum temperature distribution in a fixed bed reactor used for the oxidation of sulphur dioxide and to make calculations of the ratio between the amounts of catalyst to be used in the various stages of a multiple-stage reactor. The results of these calculations have been compared with practical experience.

Original derivation of the Mars-van Krevelen rate expression

An analysis by *M.A. Vannice / Catalysis Today 123 (2007) 18–22*

I. aromatic compound + oxidized catalyst $\xrightarrow{k_1}$ oxidation products + reduced catalyst

II. reduced catalyst + oxygen $\xrightarrow{k_2}$ oxidized catalyst

(1) the reaction in step I is first order with respect to the reactant and the fraction of sites covered by oxygen, θ;
(2) certain lattice O ions at the surface are involved in the oxidation reaction in step I;
(3) only O ions (atoms) are assumed to exist on these sites (no reactant or products);
(4) the rate of surface reoxidation (step II), i.e., O_2 adsorption, is proportional to $P_{O_2}^n$ and to the concentration of active sites not covered by oxygen, i.e., $1 - \theta$.

$$R + x\,O - S \xrightarrow{k_1} \text{Products} + x\,S \quad (2)$$

$$\left(\frac{x}{2}\right)[2S + O_2 \xrightarrow{k_2} 2O - S] \quad (3)$$

→ no elementary step, Eley-Rideal reaction very unlikely, multiple bond-breaking, multiple intermediates, sequence of elementary steps needed

→ no intermediate species of final products included, only O ions considered

where S represents an active site (a lattice surface vacancy). Their derivation is as follows [1]. From step I:

$$r_R = k_1 P_R \theta \quad (4)$$

and from step II:

$$r_{O_2} = k_2 P_{O_2}^n (1 - \theta) \quad (5)$$

→kinetic gas theory allows only $n = 1$
→ only O_2 single-site adsorption represented (two-site adsorption: $(1-\theta)^2$), however involvement of O lattice ions necessitates O_2 dissociation into atoms
→ severe inconsistency

If the oxidation of one aromatic molecule requires β molecules of O_2, then

$$r_R = \frac{r_{O_2}}{\beta} \quad (6)$$

and at steady state:

$$\beta k_1 P_R \theta = k_2 P_{O_2}^n (1 - \theta) \quad (7)$$

Consequently,

$$\theta = \frac{k_2 P_{O_2}^n}{\beta k_1 P_R + k_2 P_{O_2}^n} \quad (8)$$

Mars-van Krevelen rate equation:

$$\rightarrow \quad r_R = \frac{1}{1/k_1 P_R + \beta/k_2 P_{O_2}^n} = \frac{k_1 k_2 P_R P_{O_2}^n}{k_1 P_R + k_2 P_{O_2}^n}$$

Alternative derivations by Vannice:

Simple elementary steps for adsorption of O_2 on a lattice vacancy (active site)

$$R + O_2 - S \xrightarrow{k_1} RO_2 - S$$

$$RO_2 - S \xrightarrow{k_2} RO_2 + S$$

$$\underline{O_2 + S \xrightarrow{k_3} O_2 - S}$$

$$R + O_2 \rightarrow RO_2$$

and

$$R + O_2 - S \xrightarrow{k_1} RO + O - S$$

$$R + O - S \xrightarrow{k_2} RO + S$$

$$\underline{O_2 + S \xrightarrow{k_3} O_2 - S}$$

$$2R + O_2 \rightarrow 2RO$$

Mars-van Krevelen rate equation:

$$r_R = \frac{1}{1/k_1 P_R + \beta/k_2 P_{O_2}^n} = \frac{k_1 k_2 P_R P_{O_2}^n}{k_1 P_R + k_2 P_{O_2}^n}$$

$$\boxed{r_R = \frac{k_1 k_3 P_R P_{O_2}}{k_1 P_R + k_3 P_{O_2}}} \quad (n = 1)$$

$$\boxed{r_R = \frac{2 k_1 k_3 P_R P_{O_2}}{k_1 P_R + k_3 P_{O_2}}}$$

Simple elementary steps for **lattice O ions** involved in the reaction

$$O_2 + 2S \xrightarrow{k_1} 2O - S \quad (28)$$

$$2[R + O - S \xrightarrow{k_2} RO + S] \quad (29)$$

$$2R + O_2 \rightarrow 2RO \quad (30)$$

The rate is $r_R = k_2 P_R \theta_O$ and at steady state:

$$\frac{d[O - S]}{dt} = 2k_1 P_{O_2} \theta_v^2 - k_2 P_R \theta_O = 0 \quad (31)$$

where θ_v is the fraction of empty sites and the overall site density, L, is incorporated into k_1 and k_2. If only O atoms (ions) are included in the site balance, then

$$1 = \theta_O + \theta_v \quad (32)$$

and

$$\theta_O = \frac{2k_1 P_{O_2} (1 - \theta_O)^2}{k_2 P_R} \quad (33)$$

Mars-van Krevelen rate equation:

$$r_R = \frac{1}{1/k_1 P_R + \beta/k_2 P_{O_2}^n} = \frac{k_1 k_2 P_R P_{O_2}^n}{k_1 P_R + k_2 P_{O_2}^n}$$

?

$$r_R = k_2 P_R \left(\frac{k_2 P_R}{4 k_1 P_{O_2}} + \sqrt{\frac{k_2^2 P_R^2}{16 k_1^2 P_{O_2}^2} + 1} \right)$$

Unifying Physics and Chemistry and Catalysis; an Attempt

5. Oxidation Catalysis – Electronic Theory

Selective oxidation of hydrocarbons, consideration of bands and frontier orbitals:

$$RH + O^{2-} \rightarrow R\text{–}O^{-} + H^{+} + 2e^{-},$$

$$\tfrac{1}{2}O_2 + 2e^{-} \rightarrow O^{2-},$$

Rigid band assumption (no local surface states)

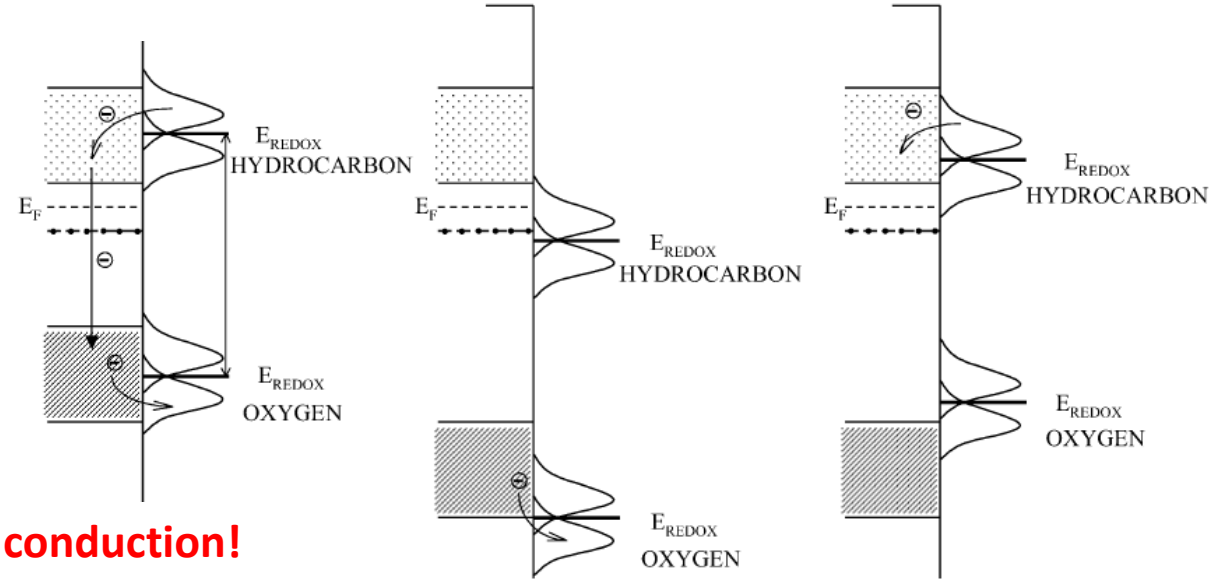

No site isolation → total conduction!

CATALYTIC OXIDATION OF HYDROCARBON MOLECULE CAN PROCEED

CATALYTIC OXIDATION OF HYDROCARBON MOLECULE CANNOT PROCEED, BECAUSE THE MOLECULE IS NOT ACTIVATED

CATALYTIC OXIDATION OF HYDROCARBON MOLECULE CANNOT PROCEED, BECAUSE THE CATALYST IS NOT REOXIDIZED

J. Haber, M. Witko, *J. Catal.* **2003**, *216*, 416-424

Surface States

Surface states of a 3D crystal

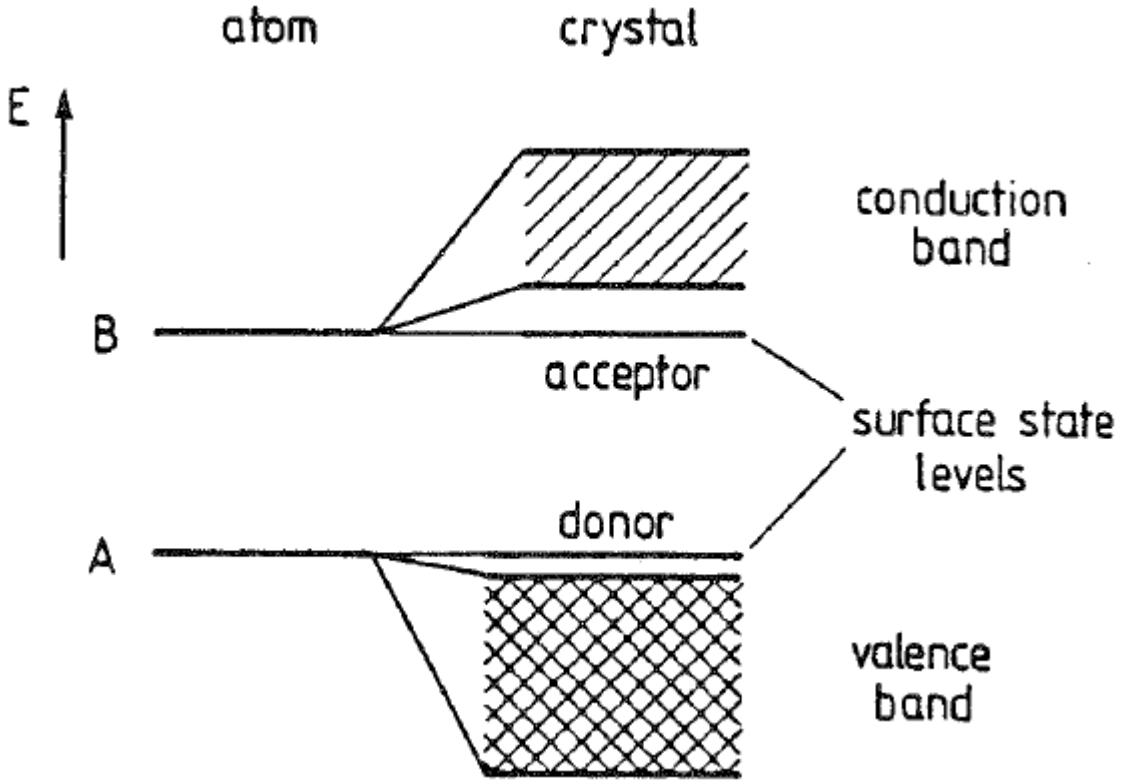

Intrinsic surface states: On ideal surfaces (perfect termination with 2D translational symmetry)

Extrinsic surface states: On surfaces with imperfections (e.g. missing atom)

H. Lüth, *Solid Surfaces, Interfaces and Thin Films*, Springer **2001**

Electrocatalytic oxidation of catechol on vanadium-doped TiO_2 electrodes

Flat band potential
(no external potential)

With external potential

Surface states

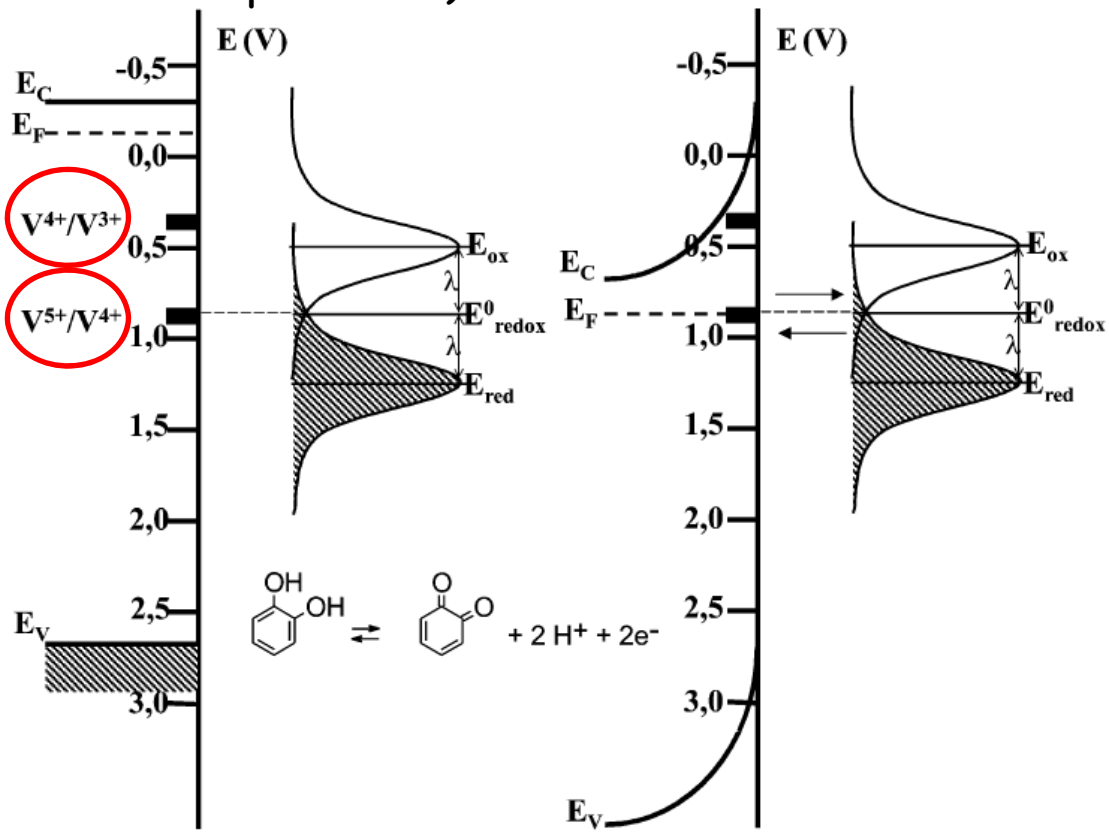

J. Haber, M. Witko, *J. Catal.* **2003**, *216*, 416-424

Hypothetical flatband situation:

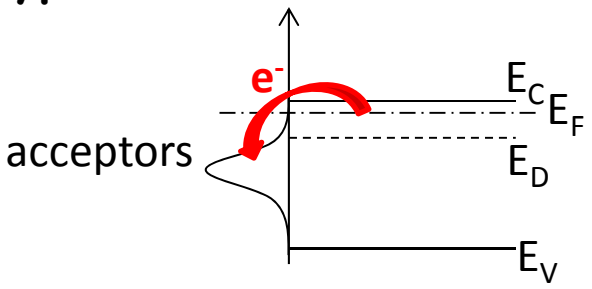

Build-up of uncompensated negative charge in surface acceptor state → unstable

Formation of (depletion) space charge layer:

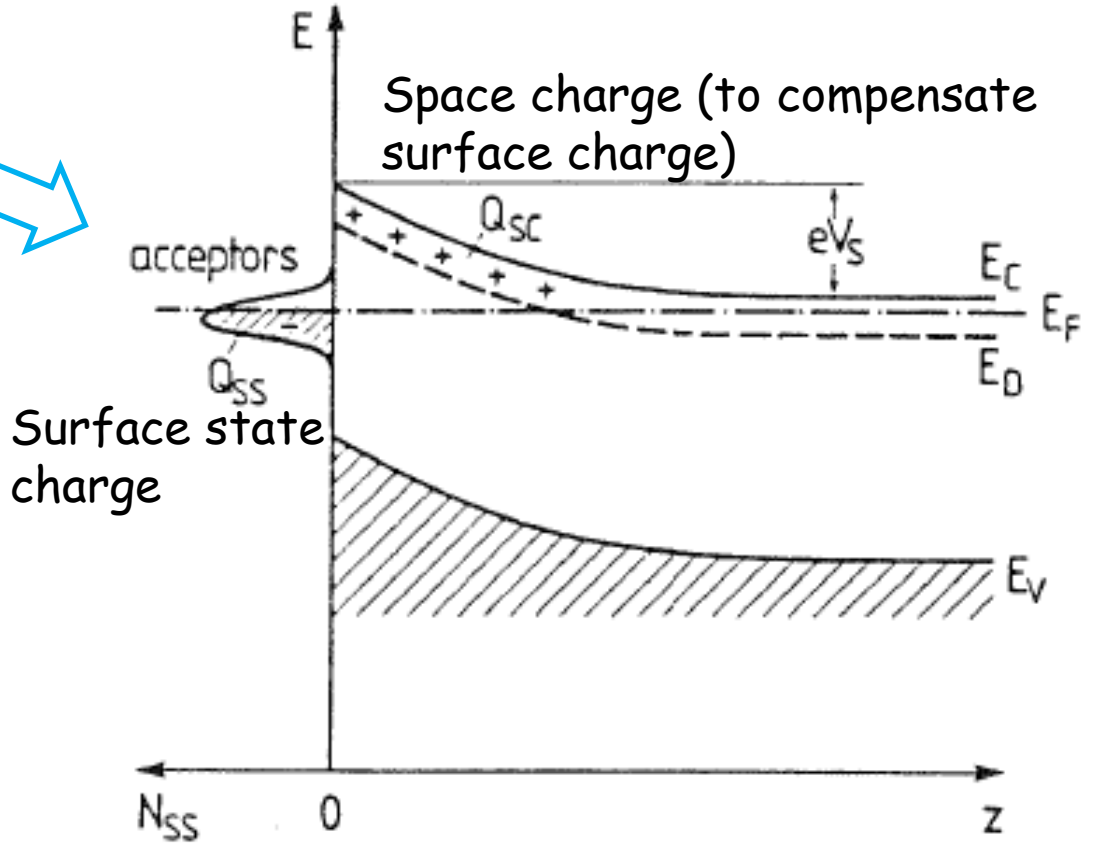

Neutrality condition $Q_{ss} = -Q_{sc}$ determines the Fermi level

H. Lüth, *Solid Surfaces, Interfaces and Thin Films*, Springer **2001**

n-SC:

p-SC:

Band schemes:

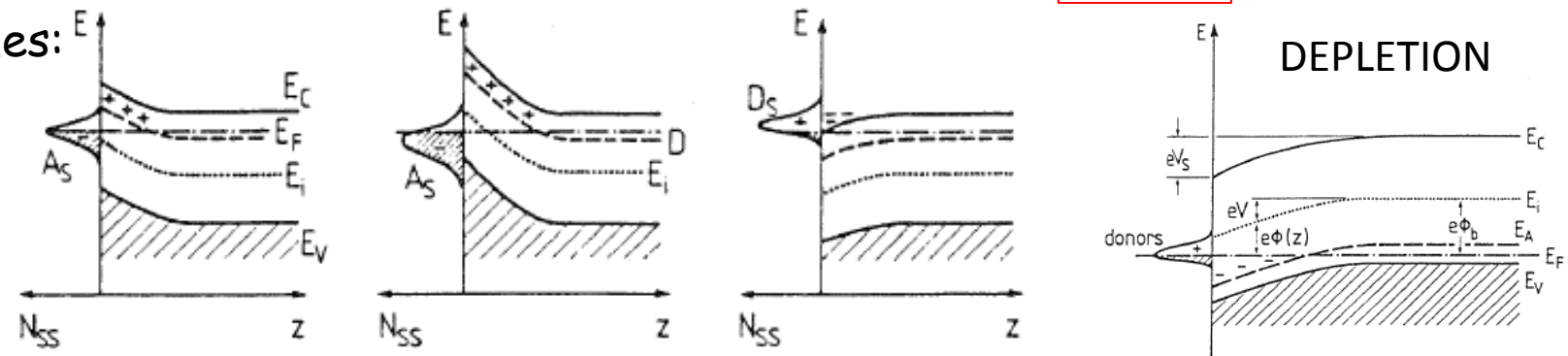

Free charge carrier densities:

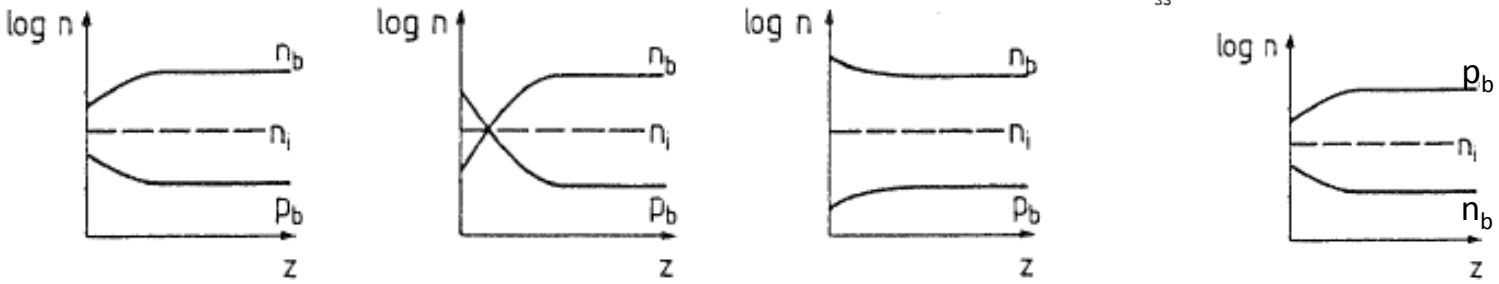

Local conductivity:

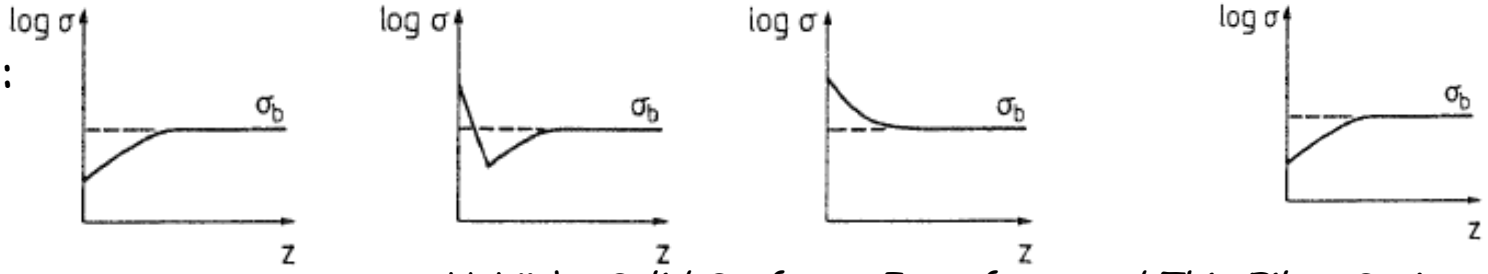

H. Lüth, *Solid Surfaces, Interfaces and Thin Films*, Springer **2001**

Adsorption (catalysis) at surface states:

p-type semiconductor (e.g. $(VO)_2P_2O_7$ for butane oxidation to maleic anhydride)

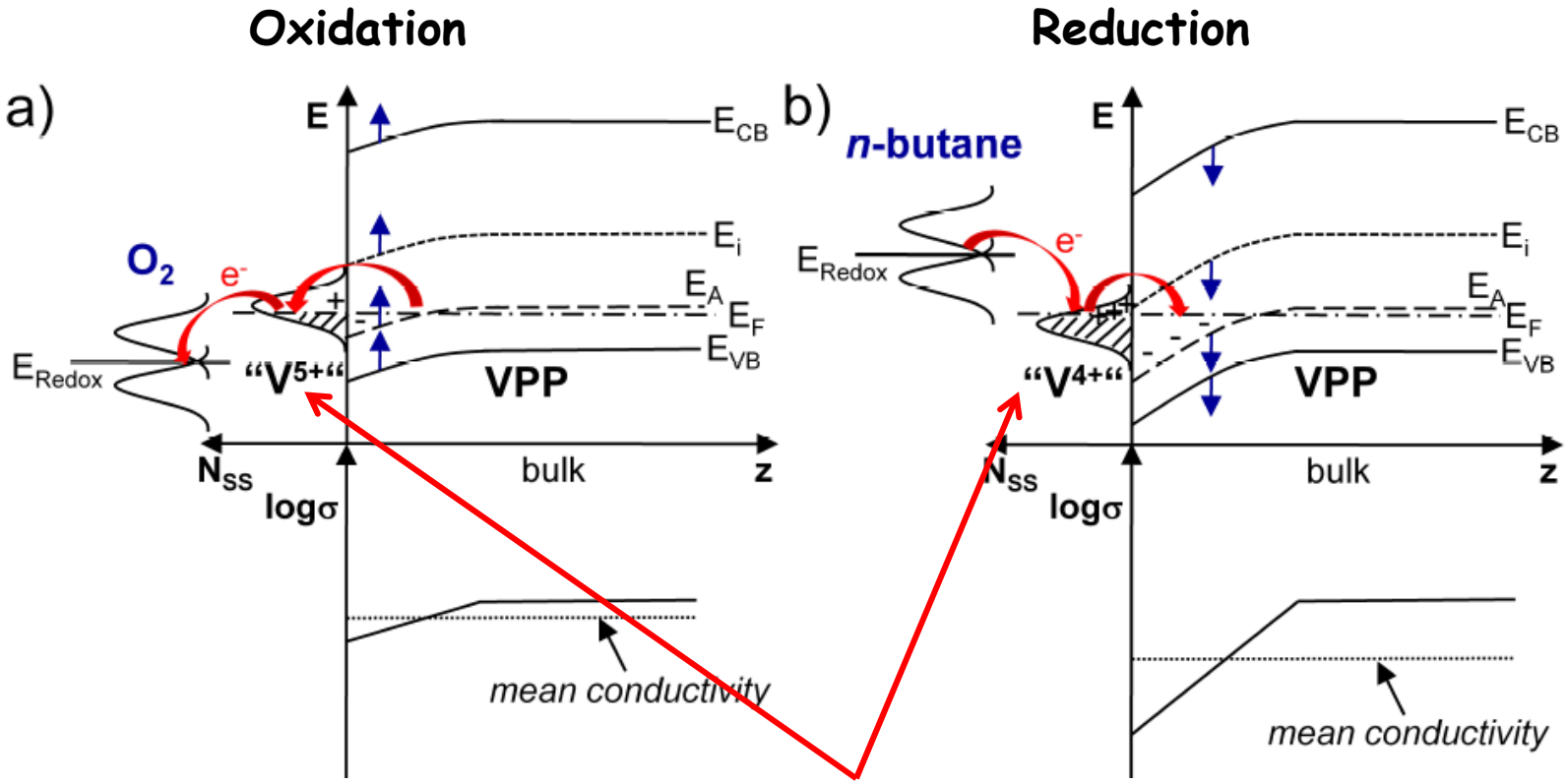

Local surface state = active (isolated single) site → selective oxidation

Spectroscopic evidence? → Photoemission spectroscopy

Core levels, valence states, work function at the surface shift by same amount of $e\Delta\Phi$ due to band bending in dependence on chemical potential of adsorbate (no surface dipoles)

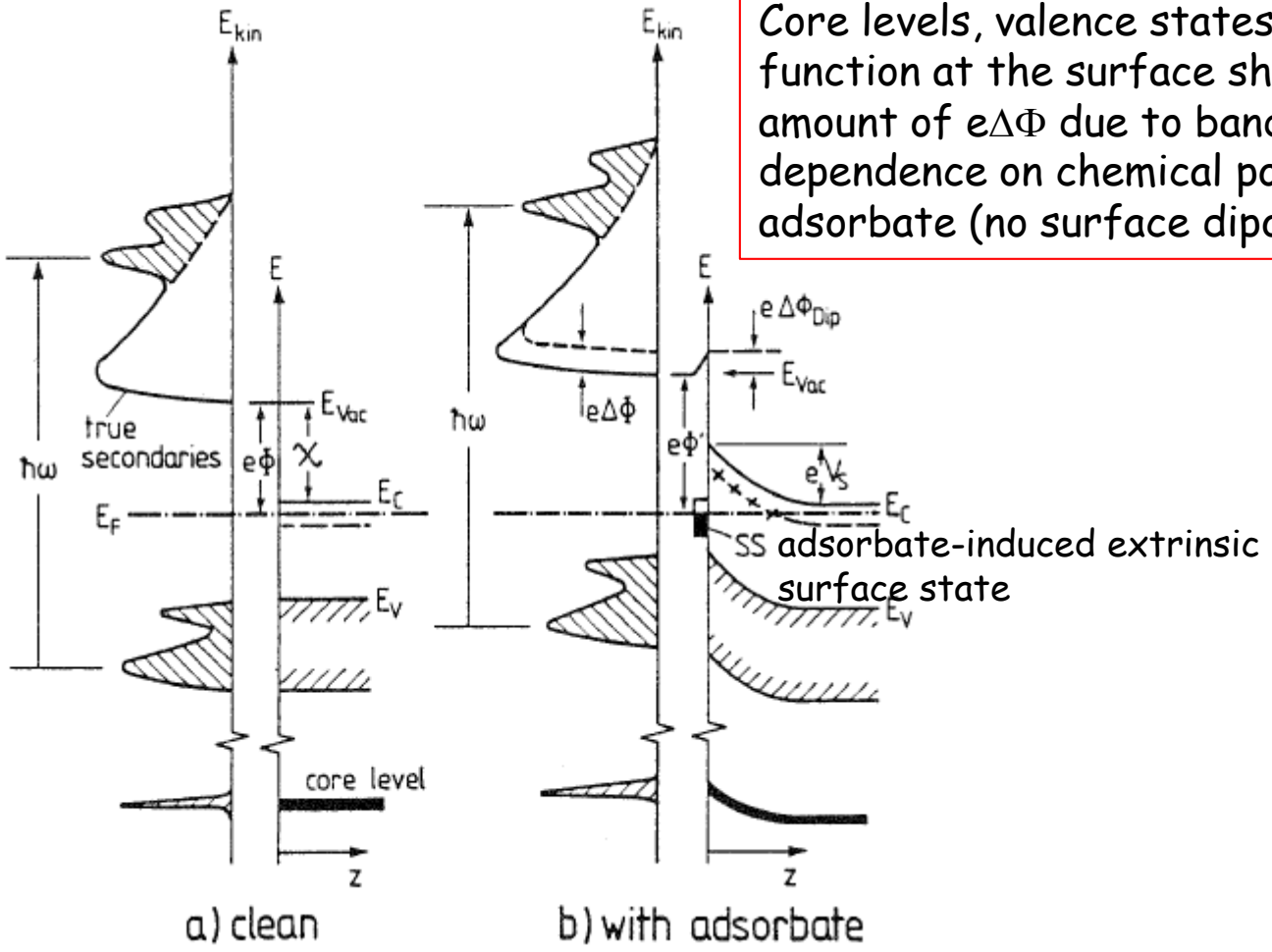

H. Lüth, *Solid Surfaces, Interfaces and Thin Films*, Springer **2001**

Valence band spectra ($h\nu$ = 35 eV) of In_2O_3 surface in dependence on P_{O2}

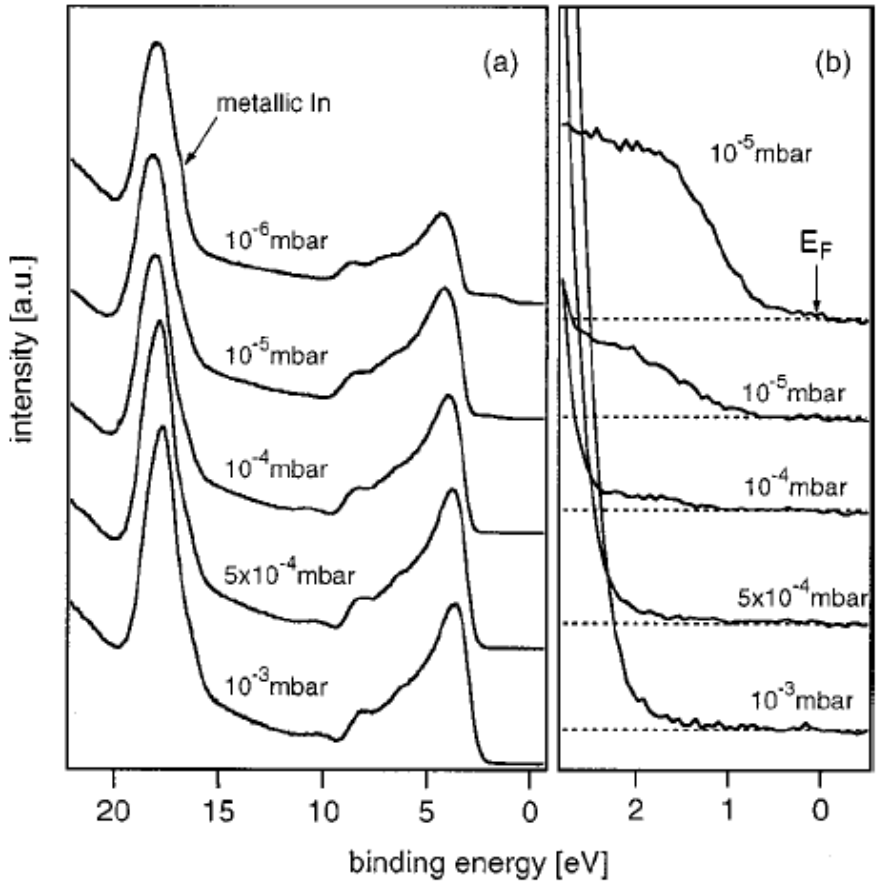

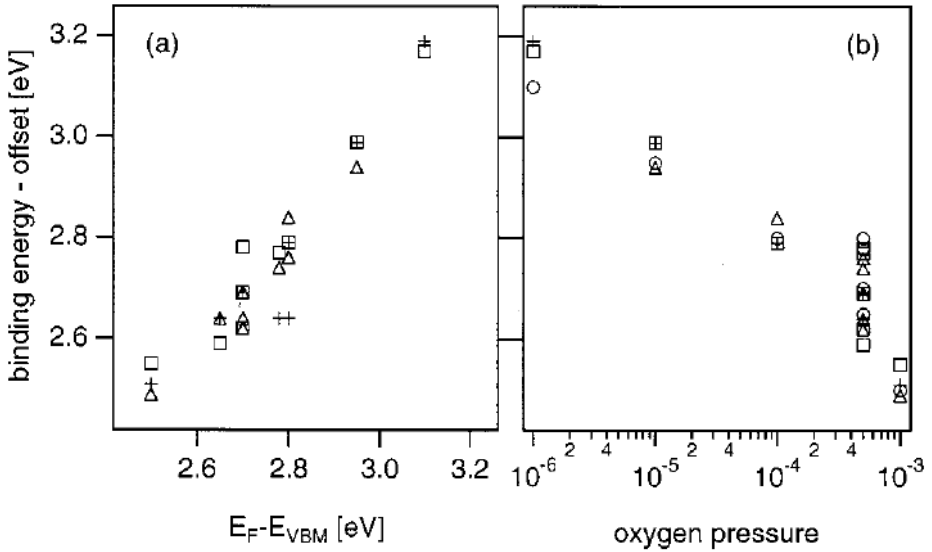

FIG. 3. Binding energies—offset of the valence band maximum (○), O 2*p* (+), secondary electron cutoff (□), and In 4*d* (△) of reactively evaporated In_2O_3 films. Offset values are 1.11 eV (O 2*p*), 13.93 eV (cutoff) and 16.16 eV (In 4*d*), respectively. The abszissa correspond to the binding energy of the valence band maximum of each film in (a) and to the oxygen pressure during deposition in (b). The parallel binding energy shifts of all levels is characteristic for a movement of the Fermi level and a constant ionization energy.

A. Klein, *Appl. Phys. Lett.* **2000**, *77*, 2009-2011

Literature

(Examples)

Reviews, e.g.:

- "*Solid state aspects of oxidation catalysis*": P. J. Gellings, H. J. M. Bouwmeester, *Catalysis Today* **2000**, *58*, 1-53; *ibid.* **1992**, *12*, 1-105
- "*The role of redox, acid-base and collective properties and of cristalline sate of heterogeneous catalysts in the selective oxidation of hydrocarbons*", J. C. Védrine, *Top. Catal.* **2002**, *21*, 97-106
- "*In situ and operando spectroscopy for assessing mechanisms of gas sensing*", A. Gurlo, R. Riedel, *Angew. Chem. Int. Ed.* **2007**, *46*, 3826-3848

Surface physics and surface chemistry, e.g.:

- S. R. Morrison, "*The chemical physics of surfaces*", Plenum Press New York and London **1977** (surface physics and surface chemistry, includes chapter on heterogeneous catalysis)
- H. Lueth, "*Solid surfaces, interfaces and thin films*", Springer **2010**
- P. A. Cox, "*The electronic structure and chemistry of solids*", Oxford University Press **1989**
- R. Hoffmann, "*Solids and surfaces : a chemist's view of bonding in extended structures*" VCH **1988**

Fundamental textbooks, e.g.:

- N. W. Ashcroft, N. D. Mermin, "*Solid state physics*", Brooks/Cole Cengage Learning **2009**
- H. Ibach, H. Lueth, "*Solid-state physics : an introduction to principles of materials science*", Springer **2009**